Chapter 7

Design for Drift and Lateral Stability

Farzad Naeim, Ph. D., S.E.
Vice President and Director of Research and Development, John A. Martin & Associates, Los Angeles, California.

Key words: Drift, P-delta, Stability, Exact methods, Approximate methods, Code provisions, UBC-97, ICBO-2000, Bent action, Chord action, Shear deformations, Moment resisting frames, Braced Frames, Shear walls, frame-wall interactions, First-order displacements, Second-order displacements.

Abstract: This chapter deals with the problems of drift and lateral stability of building structures. Design for drift and lateral stability is an issue that should be addressed in the early stages of design development. In many cases, especially in tall buildings or in cases where torsion is a major contributor to structural response, the drift criteria can become a governing factor in selection of the proper structural system. The lateral displacement or drift of a structural system under wind or earthquake forces, is important from three different perspectives: 1) structural stability; 2) architectural integrity and potential damage to various non-structural components; and 3) human comfort during, and after, the building experiences these motions. In design of building structures, different engineers attribute various meanings to the term "stability". Here, we consider only those problems related to the effects of deformation on equilibrium of the structure, as stability problems. Furthermore, we will limit the discussion to the stability of the structure as a whole. Local stability problems, such as stability of individual columns or walls, are discussed in Chapters 9, 10, and 11 of the handbook. Several practical methods for inclusion of stability effects in structural analysis as well as simplified drift design procedures are presented. These approximate methods can be valuable in evaluation of the potential drift in the early stages of design. Numerical examples are provided to aid in understanding the concepts, and to provide the reader with the "hands-on" experience needed for successful utilization of the material in everyday design practice.

7.1 INTRODUCTION

This chapter deals with the problems of drift and lateral stability of building structures. Design for drift and lateral stability is an issue which should be addressed in the early stages of design development. In many cases, especially in tall buildings or in cases where torsion is a major contributor to structural response, the drift criteria can become a governing factor in selection of the proper structural system.

In design of building structures, different engineers attribute various meanings to the term "stability"(7-1). Here, we consider only those problems related to the effects of deformation on equilibrium of the structure, as stability problems. Furthermore, we will limit the discussion to the stability of the structure as a whole. Local stability problems, such as stability of individual columns or walls, are discussed in Chapters 9, 10, and 11 of the handbook.

The concerns that have resulted in code requirements for limiting lateral deformation of structures are explained in Section 7.2. The concept of lateral stability, its relationship to drift and the P-Delta effect, and factors affecting lateral stability of structures are discussed in Section 7.3.

Several practical methods for inclusion of stability effects in structural analysis are presented in Section 7.4. Simplified drift design procedures are presented in Section 7.5. These approximate methods can be valuable in evaluation of the potential drift in the early stages of design.

Section 7.6 covers the drift and P-Delta analysis requirements of major United States seismic design codes.

Several numerical examples are provided to aid in understanding the concepts, and to provide the reader with the "hands-on" experience needed for successful utilization of the material in everyday design practice.

The relative lateral displacement of buildings is sometimes measured by an overall drift ratio or index, which is the ratio of maximum lateral displacement to the height of the building. More commonly, however, an interstory drift ratio, angle, or index is used, which is defined as the ratio of the relative displacement of a particular floor to the story height at that level (see Figure 7-1). In this chapter, unless otherwise noted, the term *drift* means the relative lateral displacement between two adjacent floors, and the term *drift index*, is defined as the drift divided by the story height.

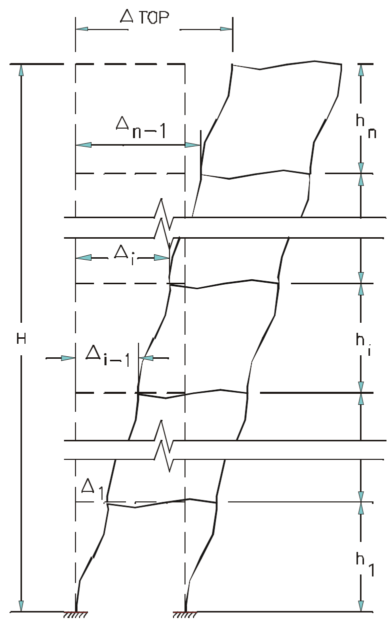

OVERALL DRIFT = Δ_{TOP}

INTER-STORY DRIFT = $\Delta_i - \Delta_{i-1}$

OVERALL DRIFT INDEX = $\dfrac{\Delta_{TOP}}{H}$

INTER-STORY DRIFT INDEX = $\dfrac{\Delta_i - \Delta_{i-1}}{h_i}$

Figure 7-1. Definition of drift.

7.2 THE NEED FOR DRIFT DESIGN

The lateral displacement or drift of a structural system under wind or earthquake forces, is important from three different perspectives: 1) structural stability; 2) architectural integrity and potential damage to various non-structural components; and 3) human comfort during, and after, the building experiences these motions.

7.2.1 Structural Stability

Excessive and uncontrolled lateral displacements can create severe structural problems. Empirical observations and theoretical dynamic response studies have indicated a strong correlation between the magnitude of interstory drift and building damage potential[7-2]. Scholl[7-3] emphasizing the fact that the potential for drift related damage is highly variable, and is dependent on the structural and nonstructural detailing provided by the designer, has proposed the following generalization of damage potential in relationship to the interstory drift index δ:

1. at $\delta = 0.001$; nonstructural damage is probable
2. at $\delta = 0.002$; nonstructural damage is likely
3. at $\delta = 0.007$; nonstructural damage is relatively certain and structural damage is likely
4. at $\delta = 0.015$; nonstructural damage is certain and structural damage is likely

Drift control requirements are included in the design provisions of most building codes. However, in most cases, the codes are not specific about the analytical assumptions to be used in the computation of the drifts. Furthermore, most of the codes are not clear about how the magnifying effects of stability related displacements ,such as P-delta deformations, are to be incorporated in evaluation of final displacements and corresponding member forces.

7.2.2 Architectural Integrity

Architectural systems and components, and a variety of other non-structural items in a building, constitute a large portion of the total investment in the project. In many cases the monetary value of these items exceeds the cost of the structural system by a large margin. In addition, these non-structural items can be potential sources of injury, and even loss of life, for building occupants and those who are in the vicinity of the building. Past earthquakes have proven that non-structural components can also greatly influence the seismic response of the building. Chapter 13 of the handbook is devoted to this important aspect of seismic design.

7.2.3 Human Comfort

Human comfort and motion perceptibility, which are of importance in the design of structures for wind induced motions, are relatively insignificant in seismic design, where the primary objective is to limit damage and prevent loss of life. For very essential structures, where continued operation of facilities is desired during and immediately after an earthquake, a more conservative design or application of special techniques, such as seismic isolation (see Chapter 14), may be considered. However, here again, the primary goal is to keep the system operational, and to prevent damage, rather than to provide for comfort of the occupants during strong ground motion.

Some investigators have studied the behavior of building occupants during strong ground motions [7-4, 7-5, 7-6]. Such studies can provide owners, architects, and hazard mitigation authorities, with valuable guidelines for considering these human factors in planning, design, and operation of building structures.

7.3 DRIFT, P-DELTA, AND LATERAL STABILITY

7.3.1 The Concept of Lateral Stability

To illustrate the concept of stability, consider an ideal column without geometrical or material imperfections. Furthermore, assume that there are no lateral loads, and that the column remains elastic regardless of the force magnitude. If the axial force is slowly increased, the column will undergo axial deformation, and no lateral displacements will occur. However, when the applied forces reach a certain magnitude called the critical load (P_{cr}), significant lateral displacements may be observed.

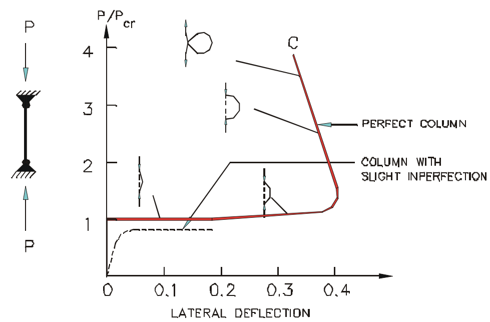

(a) LARGE DISPLACEMENT LOAD–DEFLECTION BEHAVIOR FOR AN IDEAL ELASTIC COLUMN (7–7)

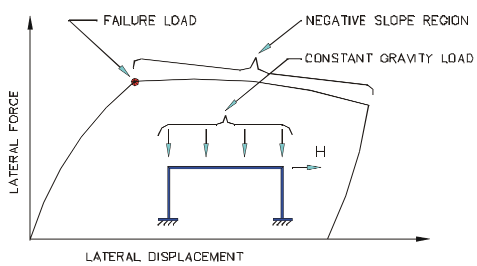

(b) LOAD–DEFLECTION RELATIONSHIP FOR A FRAME SUBJECTED TO COMBINED GRAVITY AND LATERAL LOADS

Figure 7-2. Structural stability of an idealized column and a real frame.

Figure 7-2a shows the load-deflection behavior of this ideal column. It is important to notice that when the magnitude of axial force exceeds P_{cr}, there are two possible paths of equilibrium: one along the original path, with no lateral displacements, and one with lateral displacements. However, equilibrium along the original path is not stable, and any slight disturbance can cause a change in the equilibrium position and significant lateral displacements. The force P_{cr} is called the bifurcation load or first critical load of the system. For this ideal column reaching the bifurcation point does not imply failure simply because it was assumed that it will remain elastic regardless of the deflection magnitude. However, in a real column, such large deformations can cause yielding, stiffness reduction, and failure. In a structural system, buckling of critical members and the corresponding large lateral displacements, can cause a major redistribution of forces and overall collapse of the system.

It is important to note that the bifurcation point, exists only for perfectly symmetric members under pure axial forces. If the same ideal column is simultaneously subjected to lateral loads, or if asymmetry of material or geometric imperfections are present, as they are in any real system, lateral displacements would be observed from very early stages of loading.

When a frame under constant gravity load is subjected to slowly increasing lateral loads, the lateral displacement of the system slowly increases, until it reaches a stage that in order to maintain static equilibrium a reduction in the gravity or lateral loads is necessary (Figure 7-2b). This corresponds to the region with negative slope on the force-displacement diagram. If the loads are not reduced, the system will fail.

When the same frame is subjected to earthquake ground motion, reaching the negative slope region of the load-displacement diagram, does not necessarily imply failure of the system (see Figure 7-3). In fact, it has been shown that in the case of repeated loads with direction reversals, such as those caused by earthquake ground motion, the load capacity of the system will be significantly larger than the stability load for the same system subjected to uni-directional monotonic loads[7-1, 7-8]. Perhaps this is one reason for scarcity of stability-caused building failures during earthquakes.

Exact computation of critical loads, for real buildings, is a formidable task. This is true even in a static environment, let alone the added complexities of dynamic loading and inelastic response. Exact buckling analysis is beyond the capacity and resources of a typical design office, and beyond the usual budget and time-frame allocated for structural analysis of buildings.

In everyday structural analysis, the stability effects are accounted for either by addressing the problem at the element level (via effective length factors), or by application of one of the various P-Delta analysis methods.

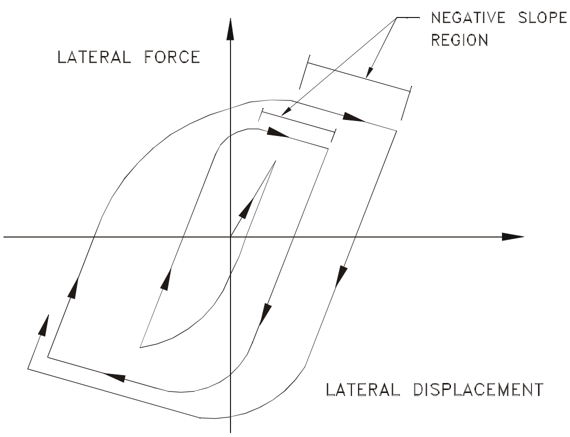

Figure 7-3. A typical load-displacement curve for a frame under constant gravity load and reversing lateral load.

The simplest way to minimize lateral stability problems is to limit the expected lateral displacement or drift of the structure. In fact several studies(7-9, 7-10, 7-11, 7-12) have shown that by increasing lateral stiffness, the critical load of the building will increase and the chances of stability problems are reduced. Drift limitations are imposed by seismic design codes primarily to serve this purpose.

7.3.2 P-Delta Analysis

For most practical purposes, an accurate estimate of the stability effects may be obtained by what is commonly referred to as P-delta analysis.

Overall stability failures of structures have not been common during past earthquakes. However, with the continuing trend towards lighter structural systems, and recent discoveries about the nature of near-field ground motion(7-13, 7-14, 7-15), the second-order effects are beginning to receive more attention. It is believed that, in most cases, observance of proper drift limitations will provide the necessary safeguard against the overall lateral

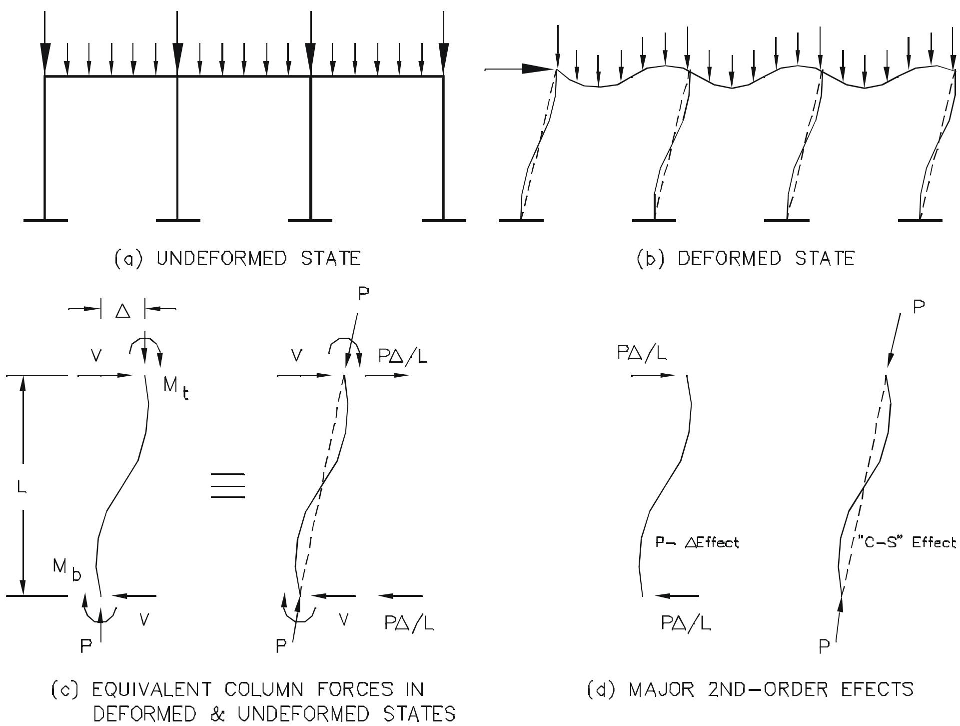

Figure 7-4. Applied loads in the undeformed and deformed states.

stability failure of the structure.

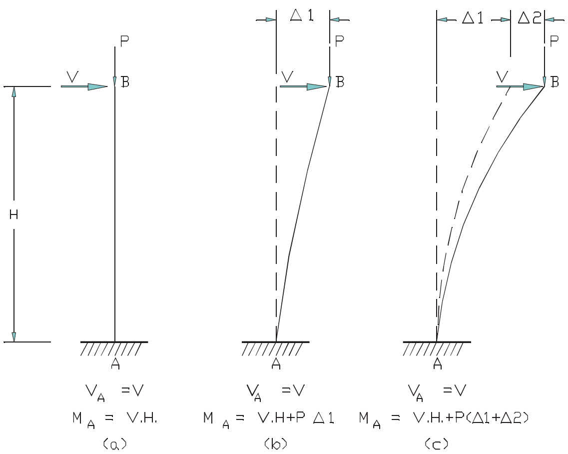

Figure 7-5. The P-delta effect. (a) Equilibrium in the under formed state. (b) Immediate P-delta effect, (c) Accumulation of the P-delta effect.

In conventional first-order structural analysis, the equilibrium equations are formulated for the undeformed shape of the structure. However, when a structure undergoes deformation, it carries the applied loads into a deformed state along with it (Fig. 7-4). The changes in position of the applied forces are cumulative in nature and cause additional second-order forces, moments, and displacements which are not accounted for in a first-order analysis. Studies(7-16) have shown that the single most important second-order effect is the P-delta effect. Figure 7-5 illustrates the P-delta effect on a simple cantilever column.

In some cases, stability or second-order effects are small and can be neglected. However, in many other cases such as tall buildings, systems under significant gravity loads, soft-story buildings, or systems with significant torsional response, the second-order effects may be quite significant and hence, should be considered in the structural analysis.

Although it is true that ignoring second-order effects is not likely to result in overall stability failure of typical buildings subjected to earthquake ground motion, these effects can frequently give rise to a series of premature material failures at the level of forces, that would seem safe by a first-order analysis. Strong evidence relating excessive drift to seismic damage during earthquakes, supports this point.

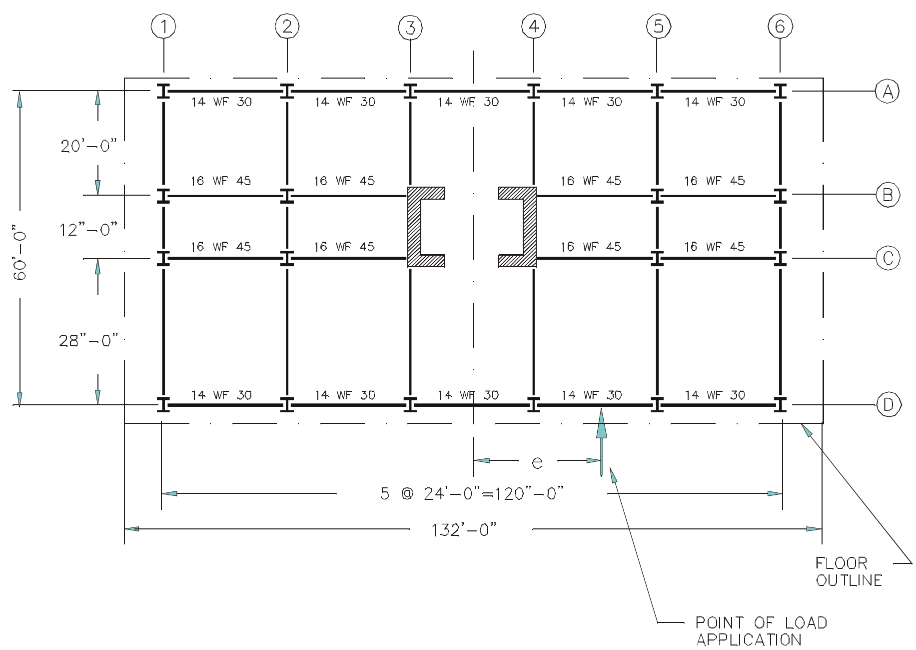

Figure 7-6. Plan of the 24 story structure (7-17).

7.3.3 Factors Affecting Lateral Stability

In general, the magnitude of the gravity loads and factors that increase lateral displacement, affect lateral stability of the structure. Chief among these factors are rotation at the base of the structure(7-12), any significant rotation at any level above the base (as that caused by formation of plastic hinges in the columns or walls), and significant asymmetry or torsion in the structure.

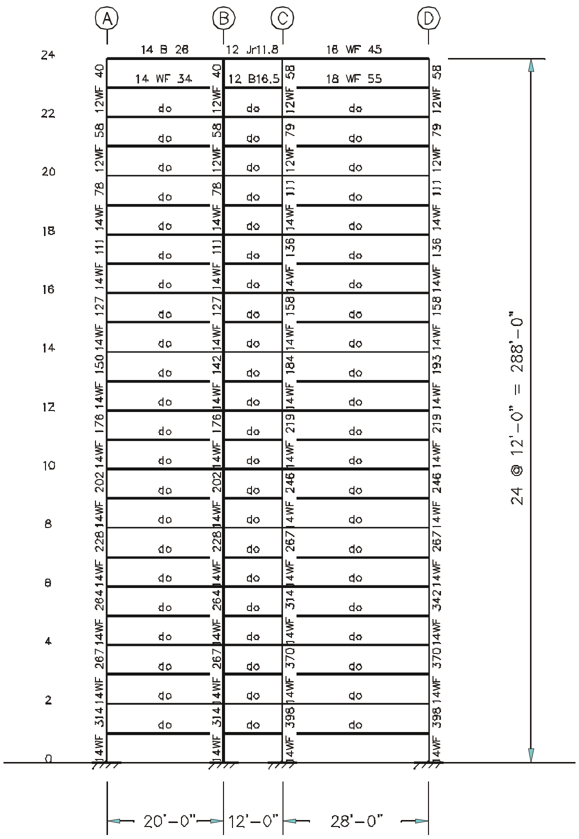

Figure 7-7. Elevation of the 24 story structure (7-17).

Wynhoven and Adams(7-17) studied the effects of asymmetry and torsion on the ultimate load carrying capacity of a 24 story frame-shear wall building with typical plan and elevation layouts as shown in Figures 7-6 and 7-7. The behavior of individual members was idealized as elastic-perfectly plastic. To consider the influence of torsion on the load carrying capacity of the structure, two asymmetric models were constructed by moving the shear-wall couple from grid lines three and four, to grid lines four and five in one model, and to grid lines five and six in another model. Load-displacement diagrams for the three configurations are shown in Figure 7-8, where λ is the ratio of the ultimate lateral loads to the working stress lateral loads. Gravity loads were not changed. Reduction in the ultimate lateral load carrying capacity due to induced asymmetry proved to be drastic (51% in one case and 66% in the other case).

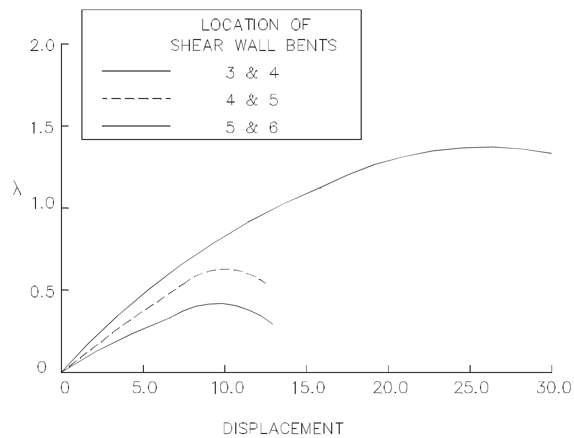

Figure 7-8. Load-displacement relationships for various configurations of the 24 story structure (7-17).

7.4 PRACTICAL SECOND-ORDER ANALYSIS TECHNIQUES

7.4.1 The Effective Length Factor Method

This method is an attempt to reduce the complex problem of overall frame stability to a relatively simple problem of elastic stability of individual columns with various end conditions. The role of the effective length factor K, is to replace an actual column of length L and complex end conditions to an equivalent column of length KL with both ends pinned, so that the classic Euler buckling equation can be used to examine column stability. It is further assumed that if the buckling stability of each individual column has been verified by this method, then a system instability will not occur.

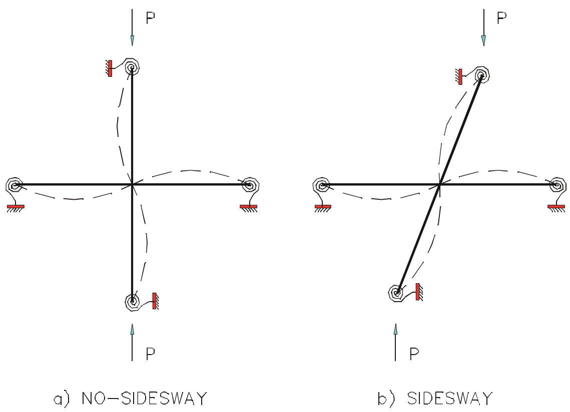

Figure 7-9. Beam-column models used in the development of the effective length factor equations.

The general equations for effective length factors are derived from the elastic stability analysis of simple beam-column models such as those shown in Figure 7-9. These equations are [(7-18)]:

for the sidesway prevented case:

$$\frac{G_A G_B}{4}\left(\frac{\pi^2}{K^2}\right)+\left(\frac{G_A+G_B}{2}\right)\left(1-\frac{\pi/k}{\tan \pi/k}\right)+\frac{2}{\pi/k}\tan\frac{\pi}{2K}=1 \tag{7-1}$$

for the sidesway permitted case:

$$\left[\frac{(\pi/K)^2 G_A G_B}{36}-1\right]\tan\frac{\pi}{K}-\left(\frac{G_A+G_B}{6}\right)\frac{\pi}{K}=0 \tag{7-2}$$

where G_A and G_B are the relative rotational stiffness of the beams to the columns, measured at ends *A* and *B* of the column under consideration:

$$G=\frac{\sum \frac{I_c}{L_c}}{\sum \frac{I_g}{L_g}} \tag{7-3}$$

Graphical solutions to these equations are given by the well known SSRC alignment charts[(7-19)] shown in Figure 7-10. The SSRC Guide[(7-19)] recommends that for pinned column bases, *G* be taken as 10, and for column bases rigidly attached to the foundation, the value of *G* be taken as unity. Furthermore, when certain conditions are known to exist at the far end of a beam, the corresponding beam stiffness term in Equation 7-3 should be multiplied by a factor. For the sidesway-prevented case, this factor is 1.5 for the far end hinged and 2.0 for the far end fixed. For the sidesway-permitted case this factor is 0.5 for the far end hinged and 0.67 for the far end fixed. Effective length factors have been incorporated in the column design interaction equations of several building design codes.

The effective-length-factor method has been subjected to serious criticism by various researchers. The main criticism is that the effective length factor method, which is based on elastic stability analysis of highly idealized cases, can not be trusted to provide reasonable estimates of the stability behavior of real structural systems. Furthermore, several studies have shown that the lateral stability of a frame, or individual story, is controlled by the collective behavior of all the columns in the story, rather than the behavior of a single column. Hence, if a stability failure is to occur, the entire story must fail as a unit[(7-12)].

Examples and evidence of the shortcomings of the effective length factor method have been documented, among others, by MacGregor and Hage[(7-16)] and Choeng-Siat-Moy[(7-20, 7-21)]. In spite of this evidence, the effective length factor method has continued to survive as a part of the requirements of many building codes. Recently, new editions of some building codes are moving away from this tradition.

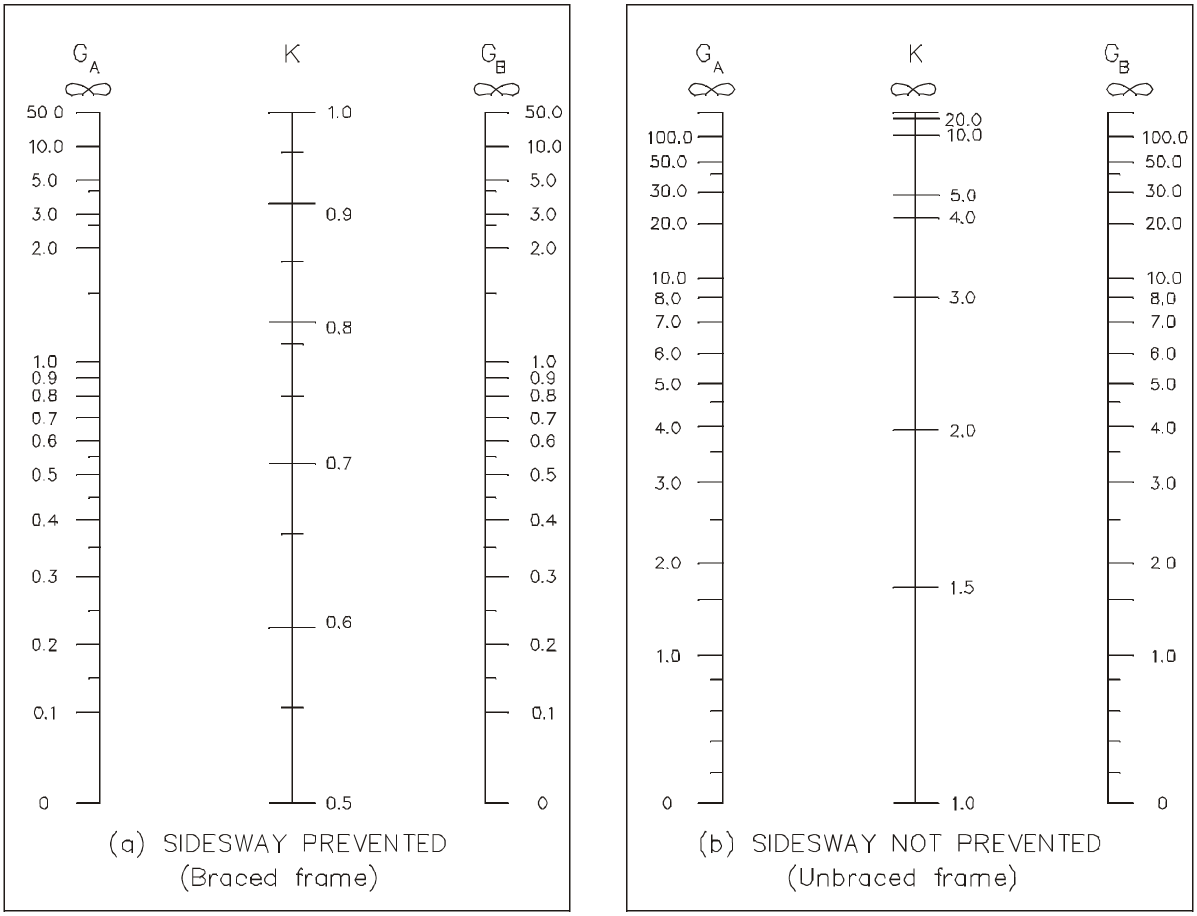

Figure 7-10. Alignment charts for determination of effective length factors[(7-19)].

7.4.2 Approximate Buckling Analysis[a]

In approximate buckling analysis, the buckling load of a single story, or that of the structure as a whole, is estimated. A magnification factor μ, which is a function of the ratio of the actual gravity load to the buckling load, is defined, and for the design of structural members, all lateral load effects are multiplied by this magnification factor. Then, member design is performed by assuming an effective length factor of one.

Several approximate methods have been developed for estimation of critical loads of building structures[(7-10, 7-11, 7-12, 7-22)]. Among these, a simple method developed by Nair[(7-22)] is explained here. This method takes advantage of the fact that most multi-story buildings have lateral load-displacement characteristics that are similar to those of either a flexural cantilever or a shear cantilever.

Buildings with braced frames or shear walls, and tall buildings with unbraced frames or tubular frames, usually have lateral load deformation characteristics that approach those of a flexural cantilever. On the other hand, buildings of low or moderate height with unbraced frames (in which column axial deformations are not significant) usually have

[a] Parts of section 7.4.2 have been extracted from Reference 6-22 with permission from Van Nostrand Reinhold Company.

lateral load-displacement characteristics similar to those of a shear cantilever.

The above observations can be extended to the torsional behavior of structures. If in a multistory building, torsional stiffness is provided by braced frames, shear walls, or tall unbraced frames not exhibiting tube action, the torsion-rotation characteristics of the building will be similar to the lateral load-displacement characteristics of a flexural cantilever. If a building's torsional stiffness is provided by low to mid-rise unbraced frames, or by tubular frames, the building will have torsion-rotation characteristics that are similar to the lateral load-displacement characteristics of a shear cantilever.

Buildings Modeled as Flexural Cantilevers

For a flexural cantilever of height H and constant stiffness EI, the uniformly distributed vertical load, per unit height (Figure 7-11), p_{cr} , that will cause lateral buckling is given by the equation

$$p_{cr} = 7.84\ EI / H^3 \tag{7-4}$$

If the stiffness varies with the equation $EI = (a/a/H)EI_0$, where EI_0 is the stiffness at the base and a is the distance from the top, the critical load is given by:

$$p_{cr} = 5.78\ EI_0/H^3 \tag{7-5}$$

If the stiffness varies with the equation $EI = (a/H)^2 EI_0$, the critical load is:

$$p_{cr} = 3.67\ EI_0 / H^3 \qquad \text{(Eq. 7-6)}$$

These solutions for critical load can be found in basic texts on elastic stability.

If a uniformly distributed lateral load of f per unit height is applied to a flexural cantilever, the lateral displacement Δ at the top is:

for a constant EI:

$$\Delta = 0.125\, f\, H^4/EI \tag{7-7}$$

for $EI = (a/H)\ EI_0$:

$$\Delta = 0.167\, fH^4/EI_0 \tag{7-8}$$

for $EI = (a/H)^2 EI_0$:

$$\Delta = 0.250\, fH^4/EI_0 \tag{7-9}$$

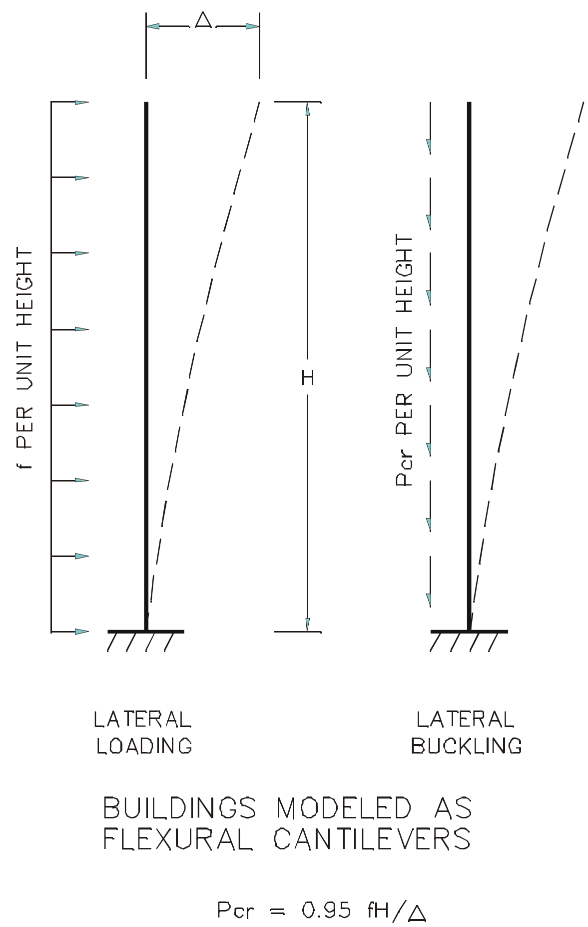

Figure 7-11. Lateral loading and buckling of a flexural cantilever[(7-22)].

If the lateral load is not uniform, an approximate answer may be obtained by defining f as the equivalent uniform lateral load that would produce the same base moment as the lateral load used in the analysis. By combining Equations 7-4, 7-5, and 7-6 with

Equations 7-7, 7-8 and 7-9, EI can be eliminated and p_{cr} can be expressed in terms of f/Δ , as follows:

for a constant EI :

$$p_{cr} = 0.98\, fH/D \tag{7-10}$$

for $EI = (a/H)\, EI_0$:

$$p_{cr} = 0.96\, fH/D \tag{7-11}$$

for $EI = (a/H\,)^2 EI_0$:

$$p_{cr} = 0.92\, fH/D \tag{7-12}$$

From the above equations it is obvious that the relation between p_{cr} and f/Δ is not very sensitive to stiffness variation over the height of the structure. Hence, regardless of the distribution of stiffness, the following equation is sufficiently accurate for design purposes:

$$p_{cr} = 0.95\, fH\,/\Delta \tag{7-13}$$

The magnification factor μ, as previously defined, is given by:

$$\mu = \frac{1}{1 - \gamma p\, /\, \phi\, p_{cr}} \tag{7-14}$$

where p is the actual average gravity load per unit height on the building, γ is the design load factor, and ϕ is the strength reduction factor. Note that p must include the load on all vertical members, including those that are not part of the lateral-load-resisting system.

Thus, if the lateral displacement is known from a first-order analysis, the critical load and the corresponding magnification factor can be estimated using Equations 7-13 and 7-14.

For buildings whose torsional behavior approaches that of a flexural cantilever, the following formula may be used to estimate the torsional buckling load of the structure:

$$r^2\, p_{cr} = 0.95\; tH\, /\, \theta \tag{7-15}$$

where t is an applied torsional load, per unit height of the building, θ is the rotation at the top of the building in radians, p_{cr} is the critical vertical load for torsional buckling per unit height of the building, and r is the polar radius of gyration of the vertical loading about the vertical axis at the center of twist of the building.

For a doubly symmetric structure, uniformly distributed gravity loading, and a rectangular floor plan with dimensions a and b:

$$r^2 = \frac{a^2 + b^2}{12} \tag{7-16}$$

Buildings Modeled as Shear Cantilevers

If a portion of a vertical shear cantilever undergoes lateral deformation δ, over a height h, when subjected to a shear force V, the critical load for lateral buckling of that portion of the cantilever is given by

$$P_{cr} = Vh/\delta \tag{7-17}$$

When the above equation is applied to a single story of a building, h is the story height, δ is the story drift caused by the story shear force V, and P_{cr} is the total vertical force that would cause lateral buckling of the story (see Figure 7-12).

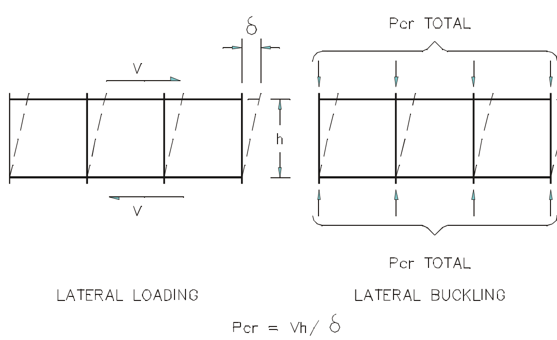

Figure 7-12. Lateral loading and buckling of a story in a shear cantilever type building(7-22).

The magnification factor μ , is given by

$$\mu = \frac{1}{1 - \gamma P / \phi P_{cr}} \qquad (7\text{-}18)$$

where P is the total gravity force in the story, γ is the load factor, and ϕ is the strength reduction factor.

The accuracy of Equation 7-17, when applied to a single story of a framed structure, depends on the relative stiffness of the beams and columns, and on the manner in which the gravity loads are distributed among the columns. The error is greatest for stiff beams and slender columns and may be as high as 20%.

For buildings whose torsional behavior approaches that of a shear cantilever, the following equation may be used to estimate the torsional buckling load of a particular story of the building:

$$r^2 P_{cr} = T h/\theta \qquad (7\text{-}19)$$

where T is an applied torsional load on the story, θ is the torsional deformation of the story (in radians) due to the torque T, h is the story height, P_{cr} is the critical load for torsional buckling of the story, and r is the polar radius of gyration of the vertical load.

Application Examples Consider the twenty story buildings shown in Figure 7-13. The buildings are analyzed using a linear elastic analysis program for a constant lateral load of 25 psf applied in the North-South direction. The East-West plan widths are 138 ft. The gravity load is assumed to be 130 psf on each floor.

For building I, the first-order displacement at the top is 0.729 ft. Using Equation 7-13:

H = 240 ft
f = 0.025(138) = 3.45 kips/ft
Δ = 0.729 ft
p_{cr} =0.95(3.45)(240)/0.729=1079 kips/ft

The estimated critical load of 1079 k/ft corresponds to 12,948 kips or 1,360 psf on each floor. The corresponding magnification factor assuming $\gamma = \phi = 1.0$, is

$$\mu = \frac{1}{1 - 130/1360} = 1.106$$

and the magnified lateral displacement at the roof is given by:

$\gamma\Delta$ = 1.106(0.729) = 0.806 ft

An elastic stability analysis of this building (7-23) indicates a critical load of 1,369 psf for North-South buckling. A large-deformation analysis for combined gravity load and North-South lateral loading indicates a roof displacement of 0.805 ft.

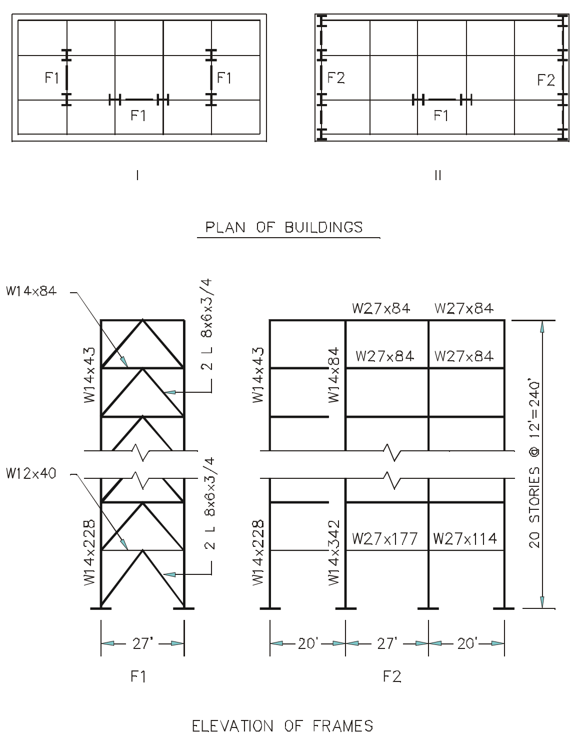

Figure 7-13. Buildings analyzed in references (7-22) and (7-23).

For building II, the computed story drifts for the 15th, 10th, and 5th levels are 0.0522 ft, 0.0609 ft, and 0.0582 ft, respectively. The corresponding story shears at these levels are 228 kips, 435 kips, and 642 kips. Using Equation 7-17:

15th story: P_{cr} = 228(12)/0.0522 = 52,414 kips

10th story: P_{cr} = 435(12)/0.0609 = 85,714 kips

5th story: P_{cr} = 642(12)/0.0582 = 132,371 kips

The corresponding magnification factors assuming $\gamma = \phi = 1.0$ are:

for the 15th story:

$$\mu = \frac{1}{1 - 7427/52{,}414} = 1.165$$

for the 10th story:

$$\mu = \frac{1}{1 - 13{,}616/85{,}714} = 1.189$$

for the 5th story:

$$\mu = \frac{1}{1 - 19{,}806/132{,}371} = 1.176$$

and the magnified story drifts are:

for the 15th story:

$\mu\,\Delta$ = 1.165(0.0522) = 0.0608 ft

for the 10th story:

$\mu\,\Delta$ = 1.189(0.0609) = 0.0724 ft

for the 5th story:

$\mu\,\Delta$ = 1.176(0.0582) = 0.0684 ft

A large-deformation analysis of this building[7-23] indicates story drifts of 0.0607 ft, 0.0723 ft, and 0.0686 ft for the 15th, 10th, and 5th stories, respectively.

7.4.3 Approximate P-Delta Analysis

Three methods for approximate P-delta analysis of building structures are presented in this section: the iterative P-delta method; the direct P-delta method; and the negative bracing member method. All three methods are shown to be capable of providing accurate estimates of P-delta effects.

Iterative P-Delta Method The iterative P-delta method[7-16, 7-24, 7-25, 7-26] is based on the simple idea of correcting first-order displacements, by adding the P-delta shears to the applied story shears. Since P-delta effects are cumulative in nature, this correction and subsequent reanalysis should be performed iteratively until convergence is achieved. At each cycle of iteration a modified set of story shears are defined as:

$$\sum V_i = \sum V_1 + \left(\sum P\right)\Delta_{i-1}/h \qquad (7\text{-}20)$$

where ΣV_i is the modified story shear at the end of ith cycle of iteration, ΣV_1 is the first-order story shear, ΣP is the sum of all gravity forces acting on and above the floor level under consideration, $\Delta_{i\text{-}1}$ is the story drift as obtained from first-order analysis in the previous cycle of iteration, and h is the story height for the floor level under consideration. Iteration may be terminated when $\sum V_i \approx \sum V_{i-1}$ or $\Delta_i \approx \Delta_{i-1}$.

Generally for elastic structures of reasonable stiffness, convergence will be achieved within one or two cycles of iteration[7-16]. One should note that since the lateral forces are being modified to approximate the P-delta effect, the column shears obtained will be slightly in error [7-16]. This is true for all approximate methods which use sway forces to approximate the P-delta effect.

EXAMPLE 7-1

For the 10 story moment resistant steel frame shown in Figure 7-14, modify the first-order lateral displacements to include the P-delta effects by using the Iterative P-delta Method. The computed first-order lateral displacements and story drifts for the frame are

Table 7-1. Applied forces and computed First-Order Displacements for the 10-story frame.

Level	Story height h, in.	Gravity force ΣP, kips	Lateral load V, kips	Story shear ΣV_1, kips	Lateral disp. D_1, in.	Story drift Δ_1, in.
10	144	180	30.22	30.22	7.996	0.517
9	144	396	21.94	52.17	7.479	0.736
8	144	612	19.57	71.74	6.743	0.785
7	144	828	17.20	88.93	5.958	0.907
6	144	1044	14.83	103.76	5.051	0.899
5	144	1260	12.45	116.21	4.152	0.914
4	144	1476	10.08	126.30	3.238	0.833
3	144	1692	7.71	134.01	2.400	0.867
2	144	1908	5.34	139.34	1.533	0.768
1	180	2124	2.97	142.31	0.765	0.765

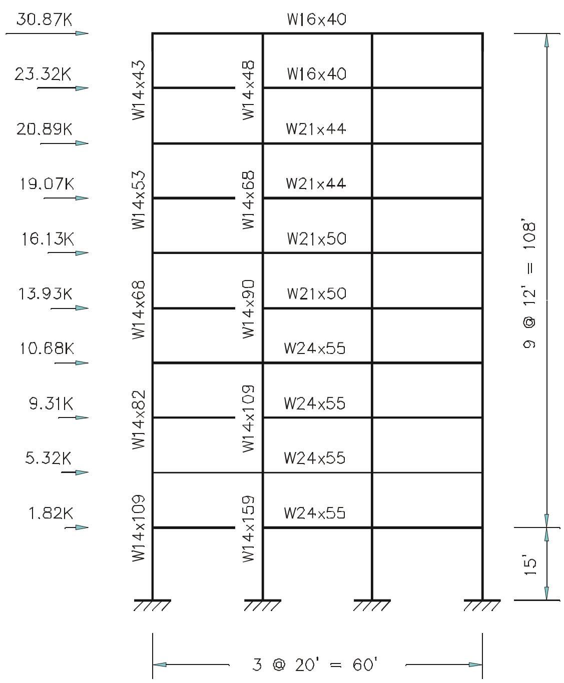

Figure 7-14. Elevation of the story moment frame used in Example 7-1.

shown in Table 7-1. The tributary width of the frame is 30 ft. The gravity load is 100 psf on the roof and 120 psf on typical floors. Use center-to-center dimensions.

The calculations for this example using the iterative P-delta method are presented in Tables 7-2 and 7-3. The convergence was achieved in two cycles of iteration. Table 7-3 also shows results obtained by an "exact" P-delta analysis.

To further explain the steps involved in the application of this method, let us consider the bent at the 8th level of the frame. The story height (h) is 12 feet (144 in.), the total gravity force at this level (ΣP) is 612 kips, the story shear (ΣV) is 71.74 kips, and the first-order story drift is 0.785 inches (see Table 7-1).

The P-Delta Contribution to the story shear is:

$$\frac{(\Sigma P)\Delta_1}{h} = \frac{(612)(0.785)}{144} = 3.34\,\text{kips}$$

and the modified story shear is:

$$\Sigma V_2 = \Sigma V_1 + (\Sigma P)\,\Delta_1 / \text{h}$$
$$= 71.74 + 3.34 = 75.08 \text{ kips}$$

Repeating this operation for all stories results in a modified set of story shears, from which a modified set of applied lateral forces is obtained (Table 7-2). A new first-order analysis of the frame subjected to these modified lateral forces results in a modified set of lateral displacements (D_2) and story drifts (Δ_2) as shown in Table 7-2. The maximum displacement obtained from the second analysis was 8.478 in., which is 9% larger than the original first-order displacement. Hence, a second iteration is necessary. Again performing the calculations for the bent at the 8th floor:

$$\frac{(\Sigma P)\,\Delta_2}{h} = \frac{(612)(0.823)}{144} = 3.50\,\text{kips}$$

$$\Sigma V_3 = \Sigma V_2 + (\Sigma P)\ \Delta_2 / h$$
$$=71.74 + 3.50 = 75.24 \text{ kips}$$

Another first-order analysis for the new set of lateral forces indicates a maximum displacement of 8.508 inches, which is less than

Table 7-2. Iterative P-delta method (First cycle of iteration)

Level	$(\Sigma P)\ \Delta_1 / h$, kips	$\Sigma V_1+(\Sigma P)\ \Delta_1 / h$, kips	Modified lateral Force V_2, kips	Modified lateral Disp. D_2, in.	Modified story Drift Δ_2, in.
10	0.65	30.87	30.87	8.478	0.533
9	2.02	54.19	23.32	7.945	0.767
8	3.34	75.08	20.89	7.178	0.823
7	5.22	94.15	19.07	6.355	0.959
6	6.52	110.28	16.13	5.396	0.955
5	8.00	124.21	13.93	4.441	0.976
4	8.59	134.89	10.68	3.465	0.897
3	10.19	144.20	9.31	2.568	0.930
2	10.18	149.52	5.32	1.638	0.823
1	9.03	151.34	1.82	0.815	0.815

Table 7-3. Iterative P-delta method (Second cycle of iteration)

Level	$(\Sigma P)\ \Delta_2 / h$, kips	$\Sigma V_2+(\Sigma P)\ \Delta_2 / h$, kips	Modified lateral Force V_3, kips	Modified lateral Disp. D_3, in.	Modified story Drift Δ_3, in.
10	0.67	30.89	30.89	8.508 (8.510)	0.534 (0.534)
9	2.11	54.28	23.39	7.975 (7.976)	0.768 (0.768)
8	3.50	75.24	20.96	7.207 (7.209)	0.825 (0.825)
7	5.51	94.44	19.20	6.382 (6.384)	0.962 (0.963)
6	6.92	110.68	16.24	5.419 (5.421)	0.959 (0.959)
5	8.54	124.75	14.07	4.461 (4.462)	0.980 (0.980)
4	9.19	135.49	10.74	3.480 (3.481)	0.900 (0.901)
3	10.93	144.94	9.45	2.580(2.581)	0.935 (0.935)
2	10.90	150.24	5.30	1.645 (1.646)	0.827 (0.827)
1	9.62	151.93	1.69	0.818 (0.819)	0.818 (0.819)

* Values in parentheses represent results of an “exact” P-delta analysis.

1% larger than the displacements obtained in the previous iteration. Hence, the iteration was terminated at this point.

The first-order and second-order lateral displacements and story drifts are shown in Figures 7-15 and 7-16. As indicated by these figures, the results are virtually identical to the exact results.

Direct P-Delta Method The direct P-delta method[7-16] is a simplification of the iterative method. Using this method, an estimate of final deflections is obtained directly from the first order deflections.

The simplification is based on the assumption that story drift at the *i*th level is proportional only to the applied story shear at that level (ΣV_i). This assumption allows the treatment of each level independent of the others.

If F is the drift caused by a unit lateral load at the *i*th level, then the first order drift Δ_1 is:

$$\Delta_1 = F\ \Sigma V_1 \tag{7-21}$$

After the first cycle of iteration,

$$\Delta_2 = F\,\Sigma V_2 = F(\Sigma V_1)\left(1+(\Sigma P)\frac{F}{h}\right) \tag{7-22}$$

and after the i th cycle of iteration:

$$\Delta_{i+1} = F\Sigma V_1\left[1+\left((\Sigma P)\frac{F}{h}\right)+\left((\Sigma P)\frac{F}{h}\right)^2 + \cdots + \left((\Sigma P)\frac{F}{h}\right)^i\right] \tag{7-23}$$

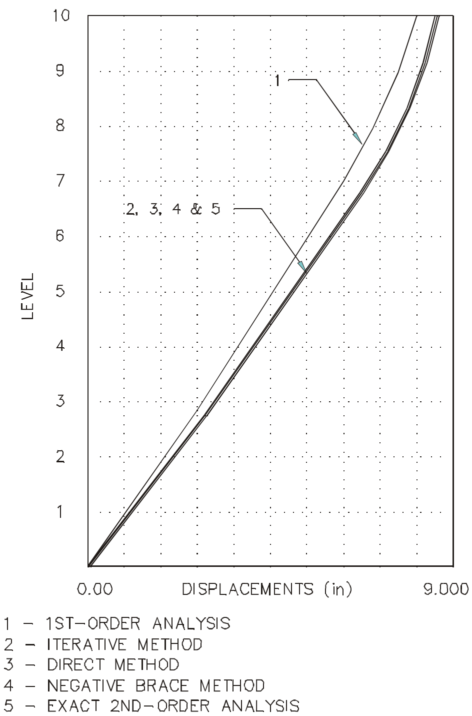

Figure 7-15. Lateral displacement of the 10-story frame as obtained by various P-delta methods.

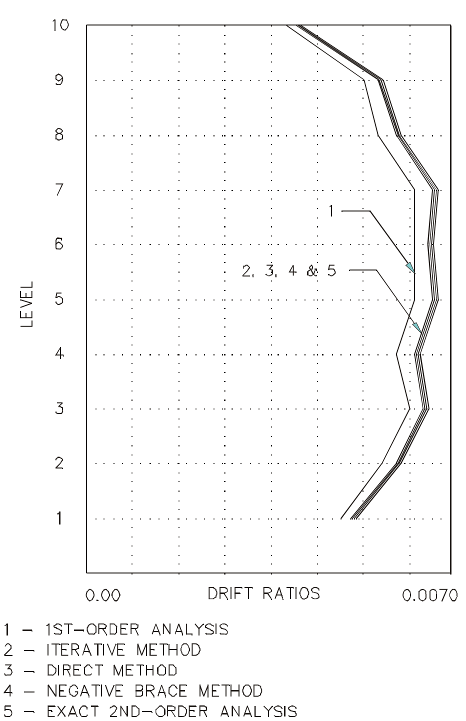

Figure 7-16. Story drift ratios of the 10 story frame as obtained by various P-delta methods.

Equation 7-23 is a geometric series that converges if $(\Sigma P)\ F/h) < 1.0$, to

$$\Delta_{Final} = \frac{F\,\Sigma V_1}{1 - F_1(\Sigma P)/h} \tag{7-24}$$

But $F\Sigma V_1 = \Delta_1$. Hence, the final second-order deflection is:

$$\Delta_{Final} = \frac{\Delta_1}{1 - (\Sigma P)\Delta_1/(\Sigma V_1)h} \tag{7-25}$$

Equation 7-25 can be expressed as $\Delta_{Final} = \mu\Delta_1$, where $\mu = 1/[1\text{-}(\Sigma P)\Delta_1/(\Sigma V_1)h]$ is a magnification factor by which the first-order effects should be multiplied to include the second-order effects. All internal forces and moments related to the lateral loads should also be magnified by μ. Member design may be carried out using an effective length factor of one.

An estimate of the critical load for an individual story, or the entire frame, can be obtained directly from Equation 7-25. Note that if $(\Sigma P)\Delta_1/(\Sigma V_1)h = 1$, the second-order displacement would go to infinity. Hence, $\Sigma P = (\Sigma V_1)h/\Delta_1$ may be considered to be the critical load of the system.

Similarly, $\Sigma(Pr^2) = \Sigma T_1\ h/\theta_1$ can be viewed as the torsional critical load of the system. It is interesting to note that the critical loads and the magnification factor obtained here are in essence the same as those obtained in Section 7.4.2. by an approximate buckling analysis.

The term $(\Sigma P)\Delta_1/(\Sigma V_1)h$ is commonly referred to as the *stability index*. Similarly, a *torsional stability index* may be defined as $\Sigma(Pr^2)\theta_1/(\Sigma T_1 h)$.

It has been suggested(7-16) that if the stability index is less than 0.0475 for all three axes of the building, the second-order effects can be ignored. For values of the stability index between 0.0475 and 0.20, the direct P-delta method can provide accurate estimates of the second-order effects. Designs for which values of the stability index exceed 0.20 should be avoided.

Table 7-4. P-delta analysis by direct P-delta method (Example 7-2)

Level	h, in	ΣV_1, kips	ΣP, kips	Δ_1, in.	μ	$\Delta_2=\mu\Delta_1$, in.	2nd-Order Disp.,in.
10	144	30.22	180	0.517	1.022	0.528	8.505
9	144	52.17	396	0.736	1.040	0.766	7.977
8	144	71.74	612	0.785	1.049	0.823	7.211
7	144	88.93	828	0.907	1.062	0.964	6.388
6	144	103.76	1044	0.899	1.067	0.959	5.424
5	144	116.21	1260	0.914	1.074	0.982	4.465
4	144	126.30	1476	0.838	1.073	0.899	3.483
3	144	134.01	1692	0.867	1.082	0.938	2.584
2	144	139.34	1908	0.768	1.079	0.829	1.646
1	180	142.31	2124	0.765	1.068	0.817	0.817

EXAMPLE 7-2

For the 10 story frame of Example 7-1 compute the second-order displacements and story drifts by the direct P-delta method.

The calculations using the direct P-delta method are shown in Table 7-4. For example, for the first floor which has a story height of 15 feet (180 inches), the story shear is 142.31 kips, the total gravity force is 2124 kips, and the first-order drift is 0.765 inches. The magnification factor and the second-order displacements are:

$$\mu = \frac{1}{1-(2124)(0.765)/(142.31)(180)} = 1.068$$

$$\Delta_2 = \mu\Delta_1 = (1.068)(0.76) = 0.817\,\text{in.}$$

A comparison with the exact results (Figures 7-15 and 7-16) reveals the remarkable accuracy of this simple technique.

Negative Bracing Member Method The negative bracing member method(7-16, 7-26, 7-27), which was first introduced by Nixon, Beaulieu and Adams(7-27), provides a direct estimate of the P-Delta effect via any standard first-order analysis program. Fictitious bracing members with negative areas are inserted (Figure 7-17) to model the stiffness reduction due to the P-delta effect.

The cross sectional area of the negative braces for each floor level can be obtained by a simple analogy to the Hooke's law ($F = K\Delta$). The additional shear due to P-delta effect is $(\Sigma P)\Delta/h$, where ΣP is the total gravity force and h is the story height. The term $\Sigma P/h$ is a stiffness term but it is contributing to lateral displacement instead of resisting it. Hence, it can be considered as a negative stiffness. A brace with a cross sectional area A, a length L_{br}, modulus of elasticity E, making an angle α with the floor, provides a stiffness equal to $(AE\text{Cos}^2\alpha)/L_{br}$ against lateral displacement. By equating the brace stiffness to $-\Sigma P/h$, the required area of the equivalent negative brace is obtained:

$$A = -\frac{\Sigma P}{h}\frac{L_{br}}{E\cos^2\alpha} \tag{7-26}$$

It is important to note that, due to the horizontal and vertical forces in the braces, the axial forces and shears in the columns will be slightly in error. These errors can be reduced by making the braces as long as possible (see Figure 7-17).

EXAMPLE 7-3

For the 10 story frame of Example 7-1, compute the second-order displacements and story drifts by the Negative Bracing Member Method. The modulus of elasticity of the braces is:

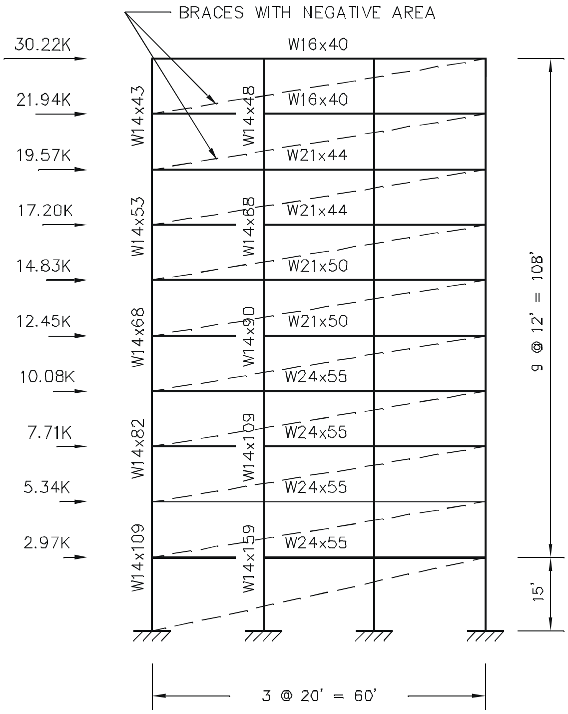

Figure 7-17. Frame modeled with negative braces.

$E = 29{,}000.$ Ksi

For a typical floor,

$$L_{br} = \sqrt{(60)^2 + (15)^2} = 61.188\,\text{ft.}$$
$$\cos^2\alpha = (60/61.188)^2 = 0.9615$$

For the first floor,

$$L_{br} = \sqrt{(60)^2 + (15)^2} = 61.847\,\text{ft.}$$
$$\cos^2\alpha = (60/61.847)^2 = 0.9412$$

The negative brace area for each floor level may now be calculated using Equation 7-26. For example, for the fourth floor where the total gravity force is 1476 kips, the negative brace area is:

$$A_4 = -\frac{(1476)(734.26)}{(144)(29000)(0.9615)} = -0.2699\,\text{in}^2$$

The brace areas, and the displacements obtained using the negative braces, are shown in Table 7-5. The very good agreement with the "exact" results (Table 7-3) is evident.

Modified Versions of Approximate P-delta Methods The P-Delta methods presented in this chapter ignore the "C-S" effect (Figure 7-4d). For most practical problems, the C-S effects are much smaller than the P-delta effects, and can be ignored. However, if needed, the P-delta methods described in previous sections, can be simply modified to include this effect.

The modification is achieved by multiplying the member axial forces by a flexibility factor, γ. For a single column, γ is given by(7-26):

Table 7-5. P-delta analysis by negative-bracing-member method.

Level	h, in	ΣP, kips	L_{br}, in.	$E\cos^2\alpha$	A_{br}, in.	2nd-Order Disp.,in.
10	144	180	734.26	27,884	-0.0329	8.458
9	144	396	734.26	27,884	-0.0724	7.929
8	144	612	734.26	27,884	-0.1120	7.168
7	144	828	734.26	27,884	-0.1514	6.350
6	144	1044	734.26	27,884	-0.1909	5.394
5	144	1260	734.26	27,884	-0.2341	4.442
4	144	1476	734.26	27,884	-0.2699	3.468
3	144	1692	734.26	27,884	-0.3094	2.572
2	144	1908	734.26	27,884	-0.3489	1.642
1	144	2124	742.16	27,295	-0.3209	0.817

$$\gamma = 1 + 0.22\frac{4(G_A - G_B)^2 + (G_A + 3)(G_B + 2)}{[(G_A + 2)(G_B + 2) - 1]^2} \tag{7-27}$$

where G_A and G_B are the stiffness ratios as defined in Section 7.4.1. The flexibility factor γ has a rather small range of variation (from 1.0 for $G_A = G_B = \infty$, to 1.22 for $G_A = G_B = 0$.). For design purposes a conservative average value of γ can be used for the entire frame. Lai and MacGregor[7-26] suggest an average value of γ = 1.15, while Stevens[7-10] has proposed an average value of γ = 1.11.

To include the C-S effect in the previously discussed P-delta methods, it is sufficient to use $\gamma\Sigma P$ instead of ΣP wherever the term ΣP appears.

EXAMPLE 7-4

For the 10-story frame of Example 7-1, compute the second-order displacements and story drifts at the first, fifth, and the roof levels by the modified direct P-delta method. An average value of γ = 1.11 is assumed for all calculations.

Using the values listed in Table 7-4 we have:

- at the roof:

$$\frac{\gamma(\Sigma P)\Delta_1}{(\Sigma V_1)h} = \frac{(1.11)(180)(0.517)}{(30.22)(144)} = 0.024$$

$$\mu = \frac{1}{1-0.024} = 1.025$$

$$\Delta_2 = \mu\Delta_1 = (1.025)(0.517) = 0.530\,\text{in.}$$

- at the fifth level:

$$\frac{\gamma(\Sigma P)\Delta_1}{(\Sigma V_1)h} = \frac{(1.11)(1260)(0.914)}{(116.21)(144)} = 0.076$$

$$\mu = \frac{1}{1-0.076} = 1.082$$

$$\Delta_2 = \mu\Delta_1 = (1.082)(0.914) = 0.989\,\text{in.}$$

- and at the first level:

$$\frac{\gamma(\Sigma P)\Delta_1}{(\Sigma V_1)h} = \frac{(1.11)(2124)(0.765)}{(142.31)(180)} = 0.070$$

$$\mu = \frac{1}{1-0.070} = 1.075$$

$$\Delta_2 = \mu\Delta_1 = (1.075)(0.765) = 0.822\,\text{in.}$$

Comparison of these results with those obtained by the original method reveals an increase of less than 1% in the story drifts due to this modification.

7.4.4 "Exact" P-Delta Analysis

Construction of the geometric stiffness matrix is the backbone of any exact second-order analysis. The same matrix is also essential for any finite element buckling analysis procedure. In this section, the concept of geometric stiffness matrix is introduced, and a general approach to "exact" second-order structural analysis is discussed.

Consider the deformed column shown in Figure 7-18. For the sake of simplicity, neglect the axial deformation of the member, and the small C-S effect. The slope deflection equations for this column can be written as[7-12]

$$M_t = \frac{EI}{L}\left(4\theta_t + 2\theta_b - \frac{6\Delta_t}{L} + \frac{6\Delta_b}{L}\right) \tag{7-28}$$

$$M_b = \frac{EI}{L}\left(2\theta_t + 4\theta_b - \frac{6\Delta_t}{L} + \frac{6\Delta_b}{L}\right) \tag{7-29}$$

From force equilibrium:

$$F_t = -\frac{M_t + M_b}{L} - \frac{P(\Delta_t - \Delta_b)}{L} \tag{7-30}$$

$$F_b = -F_t \tag{7-31}$$

Substituting Equations 7-28 and 7-29 into Equation 7-30:

$$F_t = -\frac{6EI}{L^2}(\theta_t + \theta_b) + 12\left(\frac{EI}{L^3} - \frac{P}{L}\right)(\Delta_t - \Delta_b) \tag{7-32}$$

Now if we rewrite the above equations in a matrix form, we obtain:

$$\begin{bmatrix} M_t \\ M_b \\ F_t \\ F_b \end{bmatrix} = \begin{bmatrix} \frac{4EI}{L} & \frac{2EI}{L} & -\frac{6EI}{L^2} & \frac{6EI}{L^2} \\ \frac{2EI}{L} & \frac{4EI}{L} & -\frac{6EI}{L^2} & \frac{6EI}{L^2} \\ -\frac{6EI}{L^2} & -\frac{6EI}{L^2} & \frac{12EI}{L^3} - \frac{P}{L} & -\frac{12EI}{L^3} + \frac{P}{L} \\ \frac{6EI}{L^2} & \frac{6EI}{L^2} & -\frac{12EI}{L^3} + \frac{P}{L} & \frac{12EI}{L^3} - \frac{P}{L} \end{bmatrix} \begin{bmatrix} \theta_t \\ \theta_b \\ \Delta_t \\ \Delta_b \end{bmatrix} \tag{7-33}$$

Since we wrote the equilibrium equations for the deformed shape of the member, this is a second-order stiffness matrix. Notice that the only difference between this matrix, and a standard first-order beam stiffness matrix, is the presence of *P/L* or geometric terms. The stiffness matrix given by Equation 7-33 can also be written as:

$$[K] = \lfloor K_f \rfloor - \lfloor K_g \rfloor \tag{7-34}$$

where $[K_f]$ is the standard first-order stiffness matrix (material matrix) and $[K_g]$ is the geometric stiffness matrix given by:

$$\begin{bmatrix} 0 & 0 & 0 & 0 \\ 0 & 0 & 0 & 0 \\ 0 & 0 & +P/L & -P/L \\ 0 & 0 & -P/L & +P/L \end{bmatrix}$$

Inspection of the simple second-order stiffness matrix given by Equation 7-33 shows why general second-order structural analysis has an iterative nature. The matrix includes *P/L* terms, but the axial force *P* is not known before an analysis is performed. For the first analysis cycle, *P* can be assumed to be zero (standard first-order analysis). In each subsequent analysis cycle, the member forces obtained from the previous cycle are used to form a new geometric stiffness matrix, and the analysis continues until convergence is achieved. If inelastic material behavior is to be considered, then the material stiffness matrix must also be revised at appropriate steps in the analysis.

Substantial research has been performed on the formulation of geometric stiffness matrices and finite element stability analysis of structures[7-28,7-36]. A complete formulation of the three-dimensional geometric stiffness matrix for wide flange beam-columns has been proposed by Yang and McGuire [7-36].

The common assumption that floor diaphragms are rigid in their own plane, allows condensation of lateral degrees of freedom into three degrees of freedom per floor level: two horizontal translations and a rotation about the vertical axis. This simplification significantly reduces the effort required for an "exact" second-order analysis. A number of schemes have been developed to permit direct and non-iterative inclusion of P-Delta effects in the analysis of rigid-diaphragm buildings [7-37, 7-38, 7-39].

The geometric stiffness matrix for a three dimensional rigid diaphragm building is given in Figure 7-19[7-37, 7-38]. For a three-dimensional building with *N* floor levels, $[K_g]$ is a $3N \times 3N$ matrix. For planar frames, the matrix reduces to an $N \times N$ tridiagonal matrix. The non-zero terms of this matrix are given by:

$$\alpha_i = \frac{(\Sigma P)_i}{h_i} + \frac{(\Sigma P)_{i+1}}{h_{i+1}} \tag{7-35}$$

$$\beta_i = \frac{(\Sigma T)_i}{h_i} + \frac{(\Sigma T)_{i+1}}{h_{i+1}} \tag{7-36}$$

$$\eta_i = -\frac{(\Sigma P)_i}{h_i} \quad (7\text{-}37)$$

$$\lambda_i = -\frac{(\Sigma T)_i}{h_i} \quad (7\text{-}38)$$

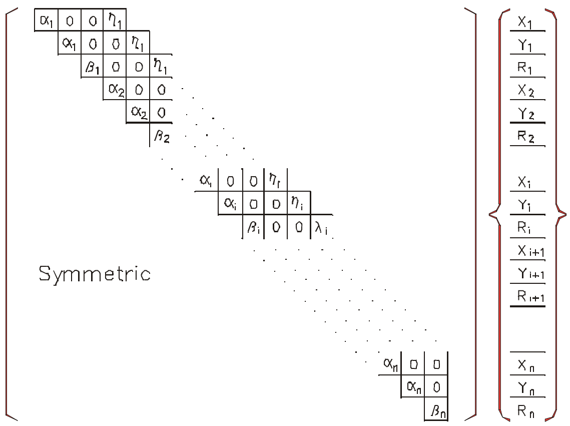

Figure 7-18. Geometric stiffness matrix for three-dimensional rigid diaphragm buildings.

where h_i is the floor height for level i, P_i is weight of the i th level, T_i is the second-order story torque, and

$$(\Sigma P)_i = \sum_{j=i}^{n} P_j \quad (7\text{-}39)$$

$$(\Sigma T)_i = \sum_{j=i}^{n} T_j \quad (7\text{-}40)$$

$(\Sigma P)_i$ can also be represented in terms of story mass, m_i, and gravitational acceleration, g, as

$$(\Sigma P)_i = \left(\sum_{j=i}^{n} m_j\right) \times g \quad (7\text{-}41)$$

The story torque, T_i, is given by [7-38]

$$T_i = \left(\sum_{j=i}^{n} p_j d_j^2\right) \frac{\theta}{h_i} \quad (7\text{-}42)$$

where p_j is the vertical force carried by the jth column, d_j is the distance of jth column from the center of rotation of the floor, and θ is an imposed unit rigid body rotation of the floor. Assuming that the dead load is evenly distributed over the floor and that a roughly uniform vertical support system is provided over the plan area of the floor, Equation 7-42 can be further simplified to

$$T_i = m_{Ri} \frac{g}{h_i} \quad (7\text{-}43)$$

where m_{Ri} is the rotational mass moment of inertia of the ith floor and g is the gravitational acceleration. The approximation involved in the derivation of Equation 7-43 is usually insignificant[7-39]. Hence, for most practical problems, Equation 7-43 can be used instead of Equation 7-42, thereby allowing the direct inclusion of the P-delta effect in a three dimensional structural analysis.

7.4.5 Choice of Member Stiffnesses for Drift and P-Delta Analysis

A common difficulty in seismic analysis of reinforced concrete structures is the selection of a set of rational stiffness values to be used in force and displacement analyses. Should one use gross concrete section properties? Should one use some reduced section properties? Or should the gross concrete properties be used for one type of analysis and reduced section properties be used for another type of analysis?

The seismic design codes in the United States are not specific about this matter. Hence, the choice of section properties used in lateral analysis in general, and seismic analysis in particular, varies widely.

Contributing to the complexity of this issue, are the following factors:

1. Although elastic material behavior is usually assumed for the sake of simplicity, reinforced concrete is not a homogeneous, linearly elastic material.
2. Stiffness and idealized elastic material properties of a reinforced concrete section vary with the state of behavior of the section (e.g. uncracked, cracked and ultimate states).

3. Not all reinforced concrete members in a structure, and not all cross sections along a particular member, are in the same state of behavior at the same time.
4. For many beams and other non-symmetrically reinforced members, the stiffness properties for positive bending and negative bending are different.
5. Stiffness of reinforced concrete members and structures varies with the time, and with the history of past exposure to wind forces and earthquake ground motions.
6. Stiffness of reinforced concrete members and structures varies with the amplitude of the applied forces.

Analytical and experimental studies[(7-40)] have indicated that for motions which are within the working stress design limits of members, the measured fundamental periods of concrete structures are generally slightly less than the periods computed using gross concrete section properties. According to Reference 7-40, in the case of large amplitude motions up to the yield level, the stiffness of the building is usually somewhere between the computed values based on the gross concrete section properties and the cracked section properties. Based on this observation, the same reference suggests that for force analysis, the gross concrete section properties and the clear span dimensions be used and the effect of nonseismic structural and nonstructural elements be considered. For drift calculations, either the lateral displacements determined using the above assumptions should be doubled or the center to center dimensions along with the average of the gross section and the cracked section properties, or one half of the gross section properties should be used. Furthermore, the nonseismic structural and nonstructural elements should be neglected, if they do not create a potential torsional reaction.

Similar sets of assumptions have been proposed by research workers who have been concerned about the choice of member stiffnesses to be used in the P-delta analysis of concrete structures. For example, for second-order analysis of concrete structures subjected to combinations of gravity and wind loads, MacGregor and Hage[(7-16)] recommend using 40% of the gross section moment of inertia for beams and 80% of the gross section moment of inertia for columns. See Chapter 15 for more information on this subject.

7.5 DRIFT DESIGN PROCEDURES

7.5.1 Drift Design of Moment Frames and Framed Tubes

The lateral displacements and story drifts of moment resistant frames and symmetrical framed tubes are caused by bent action, cantilever action, the shear leak effect, and panel zone distortions. With the simplified methods presented in this section, the contribution of each of these actions to the story drift can be estimated separately. The story drifts so obtained are then added to obtain an estimate of the total story drift. Once an estimate of the drift and the extent of the contribution of each of these actions to the total drift are known, proper corrective measures can be adopted to reduce story drifts to an acceptable level.

Bent Displacements A significant portion of drift in rigid frames and framed tubes is caused by end rotations of beams and columns (Figure 7-20). This phenomenon is commonly referred to as *bent action* (also called frame action, or racking). For most typical low to mid-rise rigid frames, almost all of the drift is caused by the bent action. However, for taller frames, other actions such as axial deformation of columns (cantilever or chord action) become more significant. For extremely tall frames, the contribution of cantilever action to drift may be several times larger than that of the bent action.

In the design of framed tubes, it is usually desirable to limit the bent action drifts to 30 to 40% of the total drift. If a framed tube is also braced, the bent action drifts are usually limited to about 20 to 25% of the total drift[(7-1)]. The bent action drift Δ_{bi} for any level i of a frame, may be estimated by[(7-41)]:

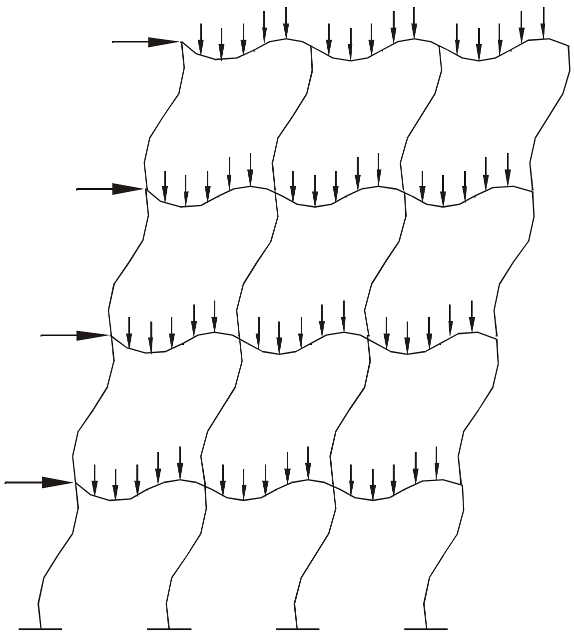

Figure 7-19. Frame deformation caused by the bent action.

$$\Delta_{bi} = \frac{(\Sigma V)_i h_i^2}{12E}\left(\frac{1}{(\Sigma K_g)_i} + \frac{1}{(\Sigma K_c)_i}\right) \quad (7\text{-}44)$$

where $(\Sigma V)_i$ is the story shear, h_i is the story height [b], and

$(\Sigma K_g)_i$ = summation of I_{gi}/L_{gi} for all girders
$(\Sigma K_c)_i$ = summation of I_{ci}/h_i for all columns
I_{gi} = individual girder moment of inertia
L_{gi} = individual bay length
I_{ci} = individual column moment of inertia

Equation 7-44 can be derived by applying the slope deflection equations to the typical subassemblage shown in Figure 7-21. In the derivation of Equation 7-44, it is assumed that the points of contraflexure are at the mid-span of beams and columns.

[b] Depending on the modeling assumption, center-to-center length, clear length, or something in between may be used.

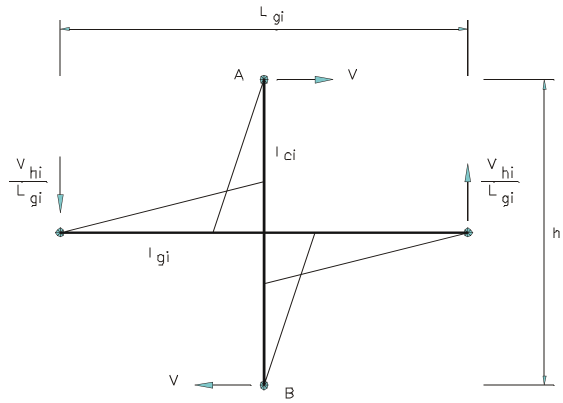

Figure 7-20. Typical subassemblage used in derivation of the bent action drift equation (7-41).

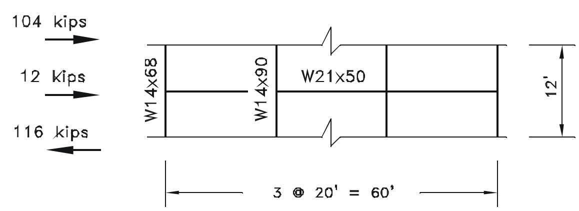

Figure 7-21. The bent at the 5th floor (Example 7-5).

Other, but similar, relationships for bent drift design have been proposed[(7-42, 7-43)]. Equation 7-44 can also be used to modify existing beam and column sizes to satisfy a given drift limit. Example 7-5 illustrates such an application.

EXAMPLE 7-5

For the bent at the 5th floor of the 10-story frame of Example 7-1 (Figure 7-22), estimate the story drift caused by bent action. Modify member sizes, if necessary, to limit the bent drift ratio to 0.0030. Neglect the P-delta effect.

W14×68	$I_{c1} = 723$ in^4
W14×90	$I_{c2} = 999$ in^4
W21×50	$I_g = 984$ in^4

$$\sum\left(\frac{I_g}{L_g}\right) = \frac{(3)(984)}{(12)(20)} = 12.30\,\text{in}^3$$

$$\sum\left(\frac{I_c}{h}\right)=\frac{(2)(723+999)}{(144)}=23.92\,\text{in.}^3$$

$$\Delta_{bi}=\frac{116(144)^2}{(12)(29000)}\left(\frac{1}{12.3}+\frac{1}{23.92}\right)$$
$$=0.85\,\text{in.}$$

$$\delta_{bi}=\frac{0.85}{144}=0.0059>0.0030 \text{ N.G.}$$

1. Increasing both beam and column sizes:

Δ_{Limit} = (0.0030)(144) = 0.432 in.

$$\Delta_{Limit}=\frac{\Delta_{bi}}{\Phi} \text{ or } 0.432=\frac{0.85}{\Phi}\rightarrow \ \Phi=1.97$$

Select new beam and column sizes:

$$I_{c1}=(1.97)(723)$$
$$=1424 \text{ in}^4 \rightarrow \text{ use W}14\times 120: I=1380\,\text{in}^4$$

$$I_{c2}=(1.97)(999)$$
$$=1968 \text{ in}^4 \rightarrow \text{use W}14\times 176: I=2140 \text{ in.}^4$$

$$I_g=(1.97)(984)$$
$$=1938 \text{ in}^4 \rightarrow \text{ use W}24\times 76: I=2100\,\text{in}^4$$

Check the new bent drift:

$$\sum\left(\frac{I_g}{L_g}\right)=\frac{(3)(2100)}{240}=26.25 \text{ in.}^3$$

$$\sum\left(\frac{I_c}{h}\right)=\frac{(2)(1380+2140)}{144}=48.89\,\text{in}^3$$

$$\Delta_{bi}=6.912\left(\frac{1}{26.25}+\frac{1}{48.89}\right)$$
$$=0.405\,\text{in.}<0.432\,\text{in.} \qquad \text{O.K.}$$

Additional member weight required for drift control:

W=3 (76-50)(20) + 2 (176+120-68-90)(12)
=4872 lb

2. Increasing beam sizes only:

$$0.432=6.912\left(\frac{1}{12.3\Phi_g}+\frac{1}{23.92}\right)\rightarrow \Phi_g=3.93$$
$$I_g=(3.93)(984)$$
$$=3867\,\text{in.}^4\rightarrow \text{ use W}30\times 99: I=3990\,\text{in}^4$$

Check the new bent drift:

$$\sum\left(\frac{I_g}{L_g}\right)=\frac{(3)(3990)}{240}=49.9\,\text{in.}^3$$

$$\Delta_{bi}=6.912\left(\frac{1}{49.9}+\frac{1}{23.92}\right)$$
$$=0.427\,\text{in.}<0.432\,\text{in.} \qquad \text{O.K.}$$

Additional member weight required for drift control:

W = 3(99-50)(20) = 2940 lb

3. Increasing column sizes only:

$$0.432=6.912\left(\frac{1}{12.3}+\frac{1}{23.92\Phi_c}\right)\rightarrow \ \Phi_c<0.$$

Therefore, bent drift control by increasing column sizes only is not feasible.

In this case, drift control by increasing beam sizes only, requires less material. However, in general, one should be careful about increasing beam sizes alone, since it can jeopardize the desirable strong column-weak girder behavior.

Cantilever Displacements In tall frames and tubes, there is significant axial deformation in the columns caused by the overturning moments. The distribution of axial forces among the columns due to the overturning moments is very similar to distribution of flexural stresses in a cantilever beam. The overturning moments cause larger axial forces and deformations on the columns which are farther from the center line of the frame. This action, which causes a lateral deformation that closely resembles the deformation of a cantilever beam (Figure 7-23), is called the cantilever or chord action. In a properly proportioned framed tube, the cantilever deflections are significantly smaller than a similar rigid frame. As shown in Figure 7-24, this is due to the participation of some of the columns in the flange frames in resistance to cantilever deformations. The taller the framed tube, the closer the column spacings, and the stronger the spandrel girders, the more significant the tube action becomes.

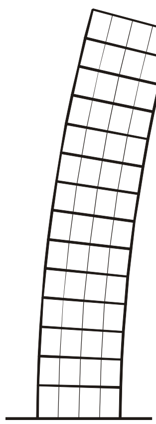

Figure 7-22. Cantilever or chord deformation.

Cantilever displacements may be estimated by simple application of the moment-area method. The moment of inertia for an equivalent cantilever beam is computed as:

$$I_{0i} = \sum (A_{ci} d_i^2) \tag{7-45}$$

where A_{ci} is cross sectional area of an individual column and d_i is its distance from the center-line of the frame. The summation is carried over all the columns of the web frames, and those columns of the flange frames which are believed to participate in resistance to cantilever deflections. The computation of cantilever displacements for each floor level can be summarized in the following steps.

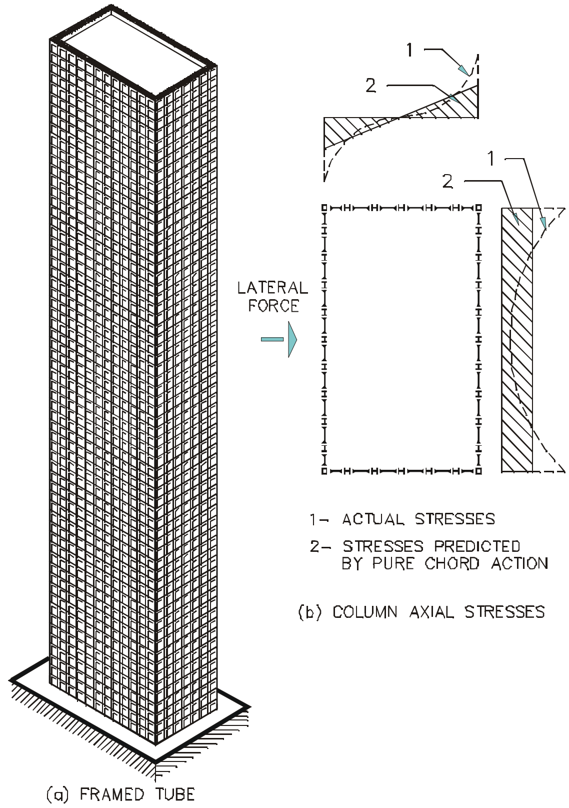

Figure 7-23. Tube action in response to lateral loads.

Step 1- Compute story moment of inertia I_{oi} using Equation 7-45.

Step 2- Compute overturning moments M_i.

Step 3- Compute Area under the M/EI_{oi} from:

$$A_i = \frac{(M_i + M_{i+1})h_i}{2EI_{0i}} \tag{7-46}$$

Step 4- Compute $\bar{x}_i$ (see Figure 7-25) from:

$$\bar{x}_i = \frac{h_i}{3}\frac{M_i + 2M_{i+1}}{M_i + M_{i+1}} \tag{7-47}$$

Step 5- Compute story displacement from:

$$\Delta_{ci} = A_i(h_i - \bar{x}_i) + \sum_{j=1}^{i-1} A_j(H_i - \bar{x}_j) \tag{7-48}$$

where H_i is the total height of the ith floor measured from the base of the structure.

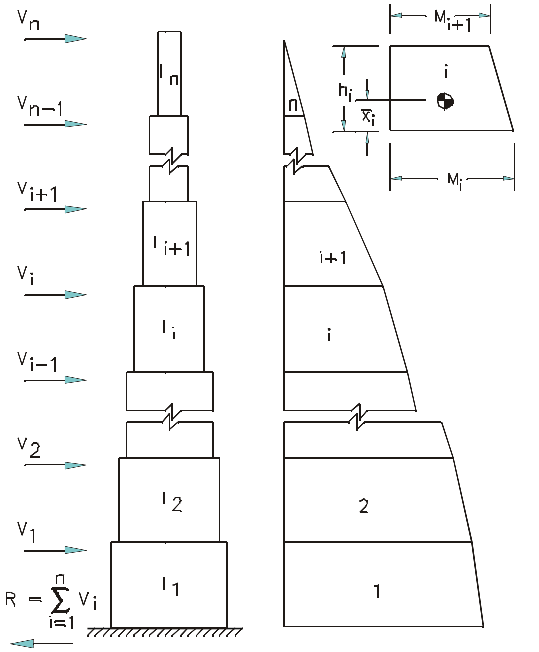

Figure 7-24. Estimating cantilever displacements by the moment area method.

EXAMPLE 7-6

Use the moment-area method and the procedure explained in this section to compute displacements at points 1, 2 and 3 of the simple cantilever column shown in Figure 7-26. Assume EI = 58 × 106, kips-in^2

Overturning moments:

$M_3 = 0.$
$M_2 = (100)(60) = 6000.$ in.-kips
$M_1 = (100)(120) = 12000.$ in.-kips
$M_0 = (100)(180) = 18000.$ in.-kips

Area under *M/EI* curve:

$A_0 = 0.$

$$A_1 = \frac{(18{,}000 + 12{,}000)(60)}{(2)(58 \times 10^6)} = 0.01552$$

$$A_2 = \frac{(12{,}000 + 6000)(60)}{(2)(58 \times 10^6)} = 0.00931$$

$$A_3 = \frac{(6000 + 0)(60)}{(2)(58 \times 10^6)} = 0.00310$$

$\bar{x}_i$ distances:

$\bar{x}_0 = 0$

$$\bar{x}_1 = \frac{(20)(18{,}000 + 24{,}000)}{18{,}000 + 12{,}000} = 28.00 \text{ in.}$$

$$\bar{x}_2 = \frac{(20)(12{,}000 + 12{,}000)}{12{,}000 + 6000} = 26.67 \text{ in.}$$

$$\bar{x}_3 = \frac{(20)(6000 + 0)}{6000 + 0} = 20.00 \text{ in.}$$

Displacements:

$$\Delta_1 = 0.01552(60 - 28) = 0.497 \text{ in.}$$

$$\Delta_2 = 0.01552(120 - 28) + 0.00931(60 - 26.67) = 1.738 \text{ in.}$$

$$\Delta_3 = 0.01552(180 - 28) + 0.00931(120 - 26.67) + 0.00310(60 - 20) = 3.352 \text{ in.}$$

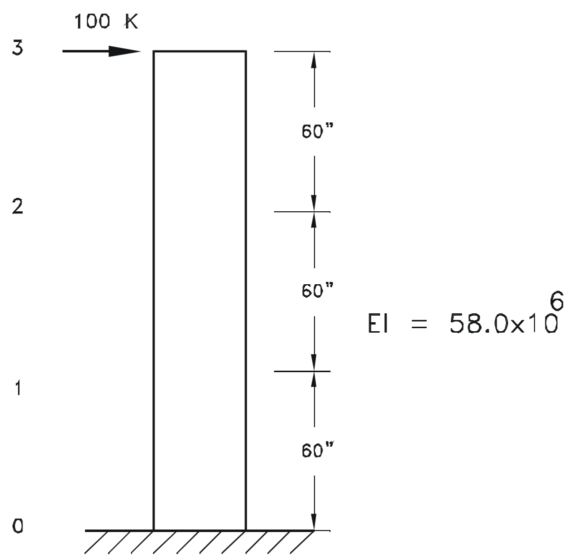

Figure 7-25. Cantilever column of example 7-6.

Shear Leak Displacements In buildings with closely spaced columns and deep girders, such as framed tubes, the contribution of shearing deformations to the lateral displacements (called the shear leak effect) may be significant. Story drifts due to the shear leak effect at level *i*, Δ_{shi}, may be estimated as [(7-41)]

$$\Delta_{shi} = \frac{\Sigma V_i h_i^2}{G}\left(\frac{1}{\Sigma A'_{gi} L_{gi}} + \frac{1}{\Sigma A'_{ci} h_i}\right) \quad (7\text{-}49)$$

where G is the shear modulus and A'_{gi} and A'_{ci} are the shear areas of individual girders and columns at level i.

In order to simplify the design process, an effective moment of inertia, I_{eff}, can be defined where the contributions of both flexural and shearing deformations are considered

$$I_{eff} = \frac{A'L^2 I}{24(1+v)I + A'L^2} \tag{7-50}$$

where A' is the shear area, L is span length, I is the moment of Inertia of the section, and v is Poisson's ratio.

EXAMPLE 7-7

For the bent of Example 7-5, estimate the additional story drift caused by the shear leak effect.

We have

W14×68: $A' = dt_w = (14.00)(0.415) = 5.83$ in.^{2}
W14×90: $A' = dt_w = (14.02)(0.440) = 6.17$ in.^{2}
W21×50: $A' = dt_w = (20.83)(0.380) = 7.92$ in.^{2}

$\Sigma A'_{gi}L_i = (3)(7.92)(240) = 5702.4$
$\Sigma A'_{ci}h_i = (2)(6.17 + 5.83)(144) = 3456.0$

Using Equation 7-49:

$$\Delta_{shi} = \frac{116(144)^2}{11{,}200}\left(\frac{1}{5702.4} + \frac{1}{3456.0}\right) = 0.10\,\text{in.}$$

Panel Zone Distortions When joint shear forces are high, and the beam-column panel zones are not adequately stiffened, panel zone distortions can have a measurable impact on the story drift. The panel zone force-deformation behavior is complex and nonlinear. Currently, there is no real consensus among researchers on appropriateness of various design-oriented approaches to this problem.

Cheong-Siat-Moy(7-44) has recommended a simple method based on elastic theory to estimate this effect. The method assumes a linear relationship between the shearing forces and the panel zone distortions. It also assumes a uniform distribution of shear stress throughout the panel zone.

A simple beam-column subassemblage and the corresponding force and displacement diagrams, as assumed by this method, are shown in Figure 7-27. It can be shown that the deformation angle γ and the additional lateral story drift due to panel zone distortion, Δ_p, are:

$$\gamma = \frac{2(M_c / d_g) - V}{Gtd_c} \tag{7-51}$$

$$\Delta_p = \frac{\gamma(h - d_g)}{2} \tag{7-52}$$

where M_c is the moment from one column, d_g is the girder depth, V is the column shear, G is the shear modulus, t is the panel zone thickness, d_c is the column depth, and h is the story height. Hence, $(h - d_g)$ is the clear column height.

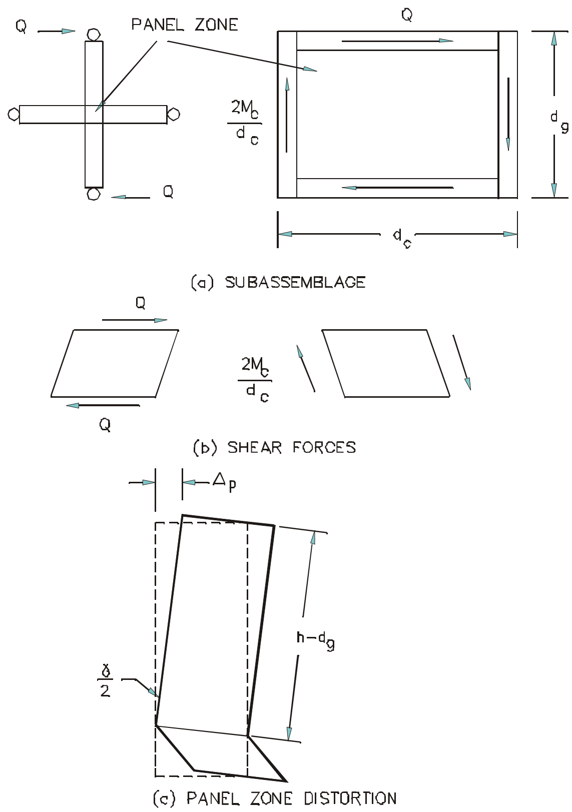

Figure 7-26. Effect of panel zone deformation(7-44)

If the points of contraflexure are assumed to be at mid-span of the beams and columns, Equation 7-51 can be further simplified to:

$$\gamma = V\frac{(h/d_g)-2}{Gtd_c} \tag{7-53}$$

Considering the approximate nature of the above formula, it is not necessary to apply it to each individual column. Instead, it can be used in an average sense (see Example 7-8).

A series of experimental and analytical studies on the behavior of steel beam-column panel zones have been conducted by various research institutions [7-45,7-46,7-47,7-48]. In one of these studies[7-48], conducted at Lehigh University, several beam-column subassemblage specimens were subjected to cyclic loads far beyond their elastic limits. Based on these tests a formula, similar to Equation 7-53, for estimation of panel zone distortions was recommended:

$$\gamma = \frac{V}{Gd_c t}\left(\frac{L_c}{d_g} - \frac{L}{h}\right) \tag{7-54}$$

where L is the beam span length, L_c is clear column length , G is the shear modulus which is taken as 11,000 ksi, and γ is the panel zone distortion in radians.

There is a serious need for further research on the seismic behavior of beam-column panel zones.

EXAMPLE 7-8

For the bent of Example 7-5, estimate the contribution of panel zone distortion to story drift assuming two conditions: a) No doubler plates, and b) $^1/_4$-in. doubler plates.

W14 × 68	d = 14.04 in	t = 0.450 in
W14 × 90	d = 14.02 in	t = 0.440 in
W21 × 50	dg = 20.83 in	

Using Cheong-Siat Moy method (Equations 7-52 and 7-53), we have

$$\gamma = V\frac{h/d_g - 2}{Gtd_c}$$

without doubler plates:

$$\text{Average } t = 2\frac{0.450+0.440}{4} = 0.445\,\text{in.}$$

Average V = 116/4 = 29 kips

$$\gamma = 29\frac{144/20.83-2}{(11200)(0.445)(14.03)} = 0.0020$$

$$\Delta_p = \gamma\frac{h-d_g}{2} = 0.0010(144-20.83)$$
$$= 0.123\,\text{in.}$$

with doubler plates:

Average t = 0.445 + 0.25 = 0.695 in

$$\Delta_p = 0.0013\frac{144-20.83}{2} = 0.080\,\text{in.}$$

Using Lehigh's formula (Equation 7-54):

$$\gamma = \frac{V}{Gd_c t}\left(\frac{L_c}{d_g} - \frac{L}{h}\right)$$

L_c= 144 - 20.83 = 123.17 in
L = 12(20) = 240 in

without doubler plates:

t = 0.445 in

$$\gamma = \frac{(29)(123.17/20.83 - 240/144)}{(11000)(14.03)(0.445)} =$$
$$0.00179\,\text{rad.}$$

Δ_p = (0.00179)(144 - 20.83)/2 = 0.110 in.

with doubler plates:

t = 0.695 in.

$$\gamma = \frac{(0.00179)(0.445)}{0.695} = 0.00115\,\text{rad.}$$

Δ_p = (0.110)(0.00115)/(0.00179) = 0.071 in.

Table 7-6. Calculation of bent-action story drifts and lateral displacements for the 10-story unbraced frame

Level	h, in.	ΣV, kips	$\Sigma(I_g/L_g)$, in.^{3}	$\Sigma(I_c/h)$, in.^{3}	Δ_{bi},in. (Eq. 7-44)	Bent Disp., in.
10	144	30.22	6.475	12.68	0.420	6.802
9	144	52.17	6.475	12.68	0.725	6.382
8	144	71.74	10.538	17.56	0.649	5.657
7	144	88.93	10.538	17.56	0.805	5.001
6	144	103.76	12.300	23.92	0.761	4.203
5	144	116.21	12.300	23.92	0.856	3.442
4	144	126.30	16.875	29.47	0.701	2.588
3	144	134.01	16.875	29.47	0.744	1.877
2	144	139.34	16.875	43.61	0.682	1.143
1	180	142.31	16.875	52.33*	0.461	0.461

* Two-thirds of the first story height was used in calculation of the bent-action drift.

Table 7-7. Calculation of shear-leak story drifts and lateral displacements for the 10-story unbraced frame.

Level	h, in.	ΣP, kips	$\Sigma(A_g{}'L_g)$, in.^{3}	$\Sigma(A_c{}'h)$, in.^{3}	Δ_{shi},in. (Eq. 7-44)	Bent Disp., In.
10	144	30.22	3516	2550	0.0379	0.8377
9	144	52.17	3516	2550	0.0653	0.7998
8	144	71.74	5206	3161	0.0675	0.7345
7	144	88.93	5206	3161	0.0837	0.6670
6	144	103.76	5999	3455	0.0893	0.5833
5	144	116.21	5999	3455	0.1000	0.4940
4	144	126.30	6703	4267	0.0897	0.3939
3	144	134.01	6703	4267	0.0951	0.3042
2	144	139.34	6703	5379	0.0864	0.2091
1	180	142.31	6703	5379	0.1226	0.1226

Drift Design of a 10 Story Moment Resistant Frame

In this subsection the approximate methods for drift and P-delta analysis which were explained previously, are put into practice by performing a complete drift design for the 10-story moment resistant steel frame introduced in Example 7-1. The goal is to achieve an economical design that meets the story drift index limitation of 0.0033.

The first step is to estimate the lateral displacements and story drifts of the structure. Calculations of story drifts and lateral displacements due to bent action, the shear leak effect, and chord action are presented in Tables 7-6, 7-7 and 7-8 respectively. It was demonstrated in Example 7-8 that the contribution of panel zone deformations to story drifts for this structure, at the level of forces considered here, is not significant. Therefore, this effect is ignored in subsequent analyses.

The total displacements and story drifts are magnified using the direct P-delta Method. These calculations are shown in Table 7-9. Notice that in sizing the members for strength, all lateral load related forces and moments should also be multiplied by the corresponding story magnification factors (see μ in Table 7-9). Once the internal forces are thus magnified, it is rational to design the members using an equivalent length factor of one.

Figures 7-28 and 7-29 depict the contribution of each action to the total lateral displacement and story drift. The dominance of bent action in the lateral response of this frame can be clearly seen in these figures. As explained previously, if the frame was significantly taller, bent action would be

Table 7-8. Calculation of chord-acrtion and lateral displacements for the 10-story unbraced frame

Level	h, in.	ΣV kips	M_{ov},[a] in-kips	I_{oi}, in^4	A,	$\bar{x}$ in.	Chord disp. in.	Chord drift, in.
10	144	30.22	4,352	3,672,000	0.294×10^5	48.00	0.5746	0.0722
9	144	52.17	11,864	3,672,000	1.096×10^5	60.88	0.5024	0.0774
8	144	71.74	22,194	4,619,520	1.830×10^5	64.72	0.4250	0.0838
7	144	88.93	35,001	4,619,520	3.074×10^5	66.63	0.3412	0.0795
6	144	103.76	49,942	5,947,200	3.546×10^5	67.78	0.2617	0.0777
5	144	116.21	66,677	5,947,200	4.868×10^5	68.56	0.1840	0.0664
4	144	126.30	84,864	7,168,320	5.249×10^5	69.12	0.1176	0.0557
3	144	134.01	104,161	7,168,320	6.547×10^5	69.55	0.0619	0.0366
2	144	139.34	124,226	9,639,360	5.882×10^5	69.89	0.0253	0.0171
1	180	142.31	149,841	9,639,360	8.824×10^5	87.20	0.0082	0.0082

[a] Overturning moment.

Table 7-9. Calculation of total first and second order story drifts and lateral displacements for the 10-story unbraced frame

Level	h, in.	ΣV, kips	ΣP, kips	Δ_1 in.	μ	$\Delta_2 = \mu\,\Delta_1$ in.	2nd –Order Disp.,in.
10	144	30.22	180	0.517	1.022	0.528	8.547
9	144	52.17	396	0.849	1.047	0.889	8.019
8	144	71.74	612	0.773	1.048	0.810	7.130
7	144	88.93	828	0.941	1.065	1.002	6.320
6	144	103.76	1044	0.898	1.067	0.958	5.318
5	144	116.21	1260	0.987	1.080	1.066	4.360
4	144	126.30	1476	0.833	1.073	0.894	3.294
3	144	134.01	1692	0.865	1.082	0.936	2.400
2	144	139.34	1908	0.786	1.081	0.850	1.464
1	180	142.31	2124	0.584	0.614	0.614	0.614

replaced by chord action as the dominant contributor to lateral displacement.

The results of this approximate analysis are compared to the results of an exact elastic analysis in Figures 7-30 and 7-31, where the good agreement between the two sets of results may be observed.

Given the dominance of bent action in this case, a simple drift design strategy based on reducing the bent drift is adopted. The maximum bent drift is about 80% of the maximum total drift. Hence, it would be rational to reduce the bent drift ratios to 80% of the maximum allowable value of 0.0033 (≈ 0.0026). It should be noted that increasing member sizes would further reduce the contribution of chord and shear leak actions to the drift. Assuming that the drift control is to be achieved by increasing both beam and column sizes, the average magnification factors *Φ* by which the moment of inertia of beams and columns should be multiplied can be calculated as described in part 1 of Example 7-5. Based on the average values of **Φ**, new member sizes for beams and columns are selected. These member sizes are shown in Figure 7-32, where the computed values of **Φ** are shown in parenthesis.

At this stage, another round of displacement analysis, similar to that performed in Tables 7-6 to 7-9, is necessary to make sure that the new design satisfies the drift design criteria. Results of this analysis are shown in Figures 7-33 and 7-34, which indicate that the new design satisfies the design drift criteria. This was also confirmed by performing an exact structural analysis (Figures 7-35 and 7-36).

The last item on the agenda, is to check the satisfaction of the strength criteria by the new design. Codified equivalent static lateral forces, which are based on a pre-determined fundamental period for the structure, do not necessarily change with variation of stiffness.

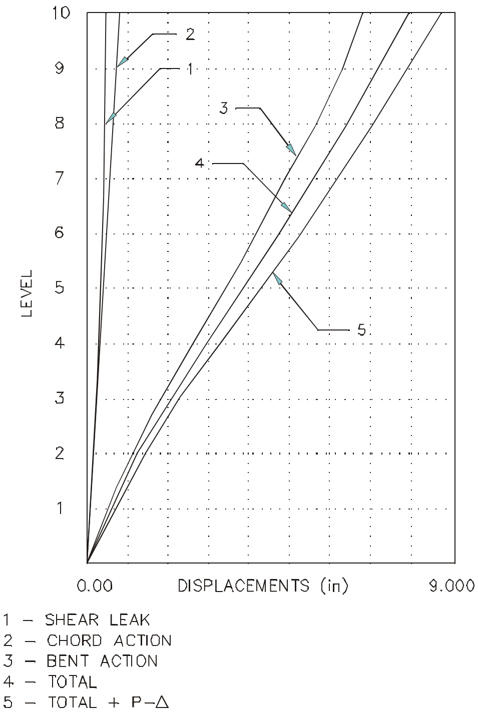

Figure 7-27. Contribution of various actions to the total lateral displacement of the 10 story frame.

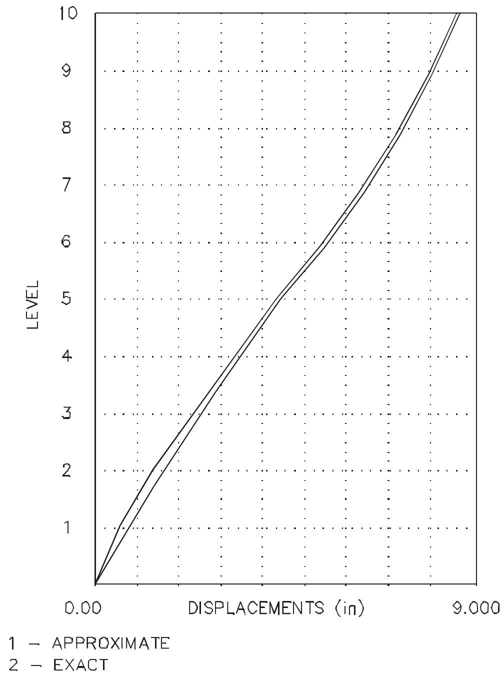

Figure 7-29. Comparison of approximate and “exact” second-order displacements.

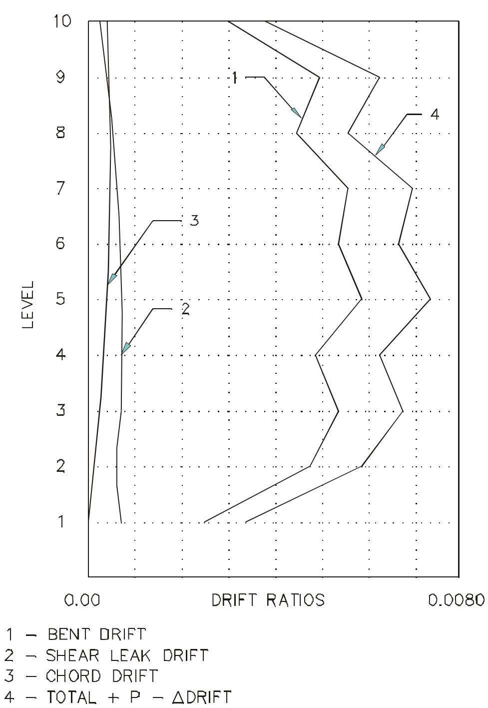

Figure 7-28. Contribution of various actions to the total interstory drift ratios of the 10 story frame.

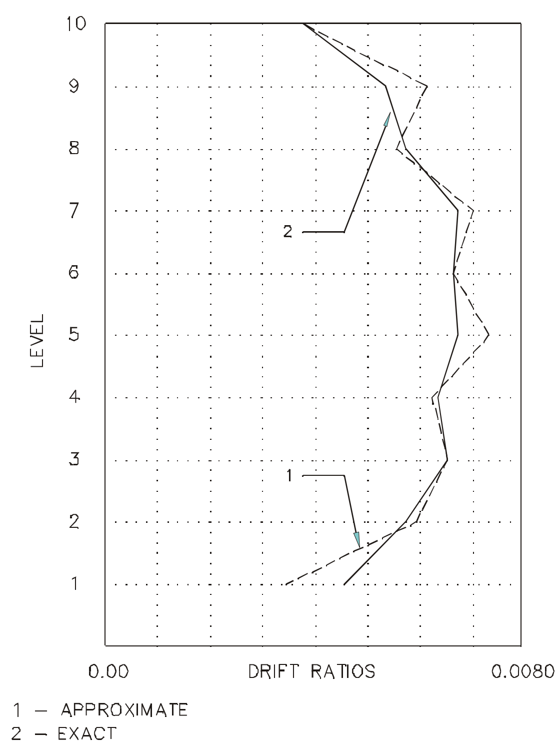

Figure 7-30. Comparison of approximate and “exact” second-order interstoy drift ratios.

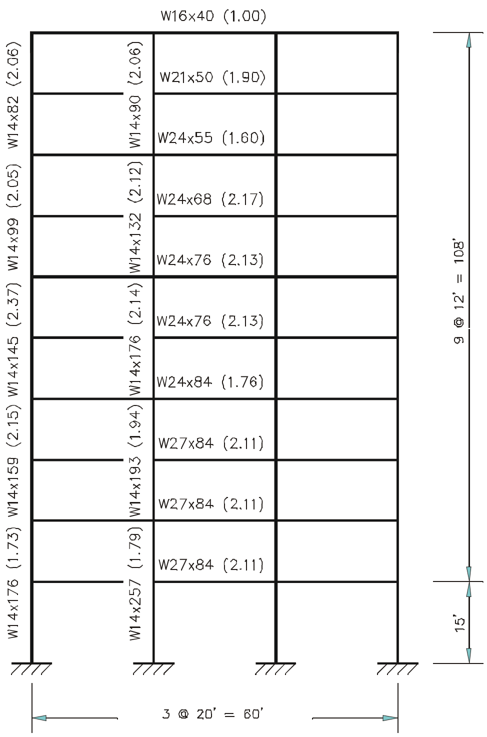

Figure 7-31. Member sections after drift design.

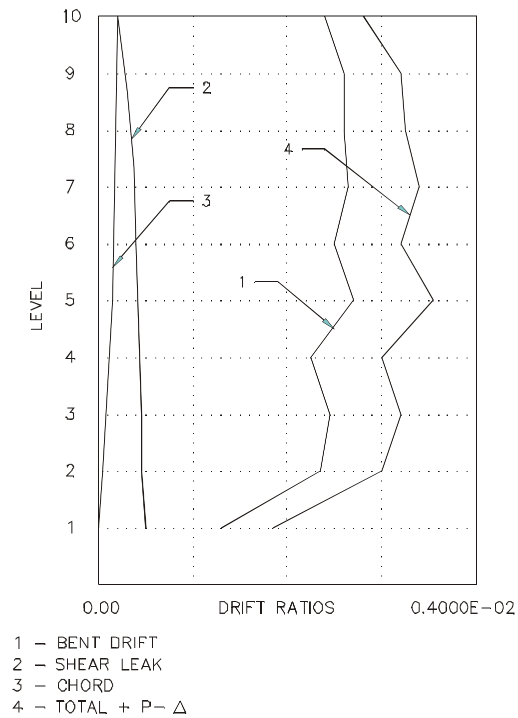

Figure 7-33. Approximate interstory drift ratios for the 10 story frame after drift design.

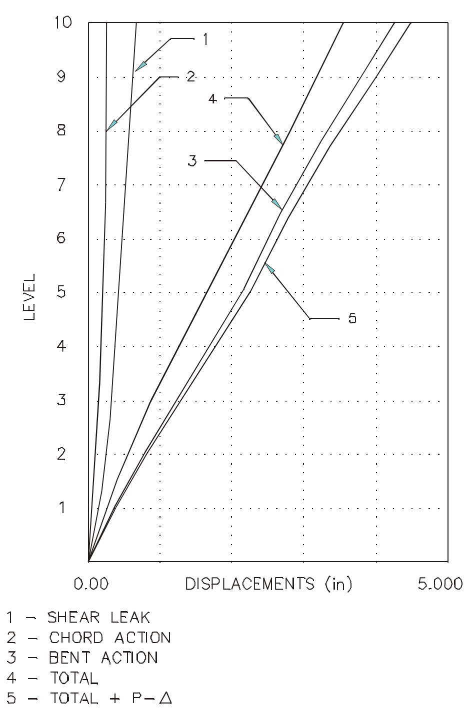

Figure 7-32. Approximate lateral displacements for the 10 story frame after drift design.

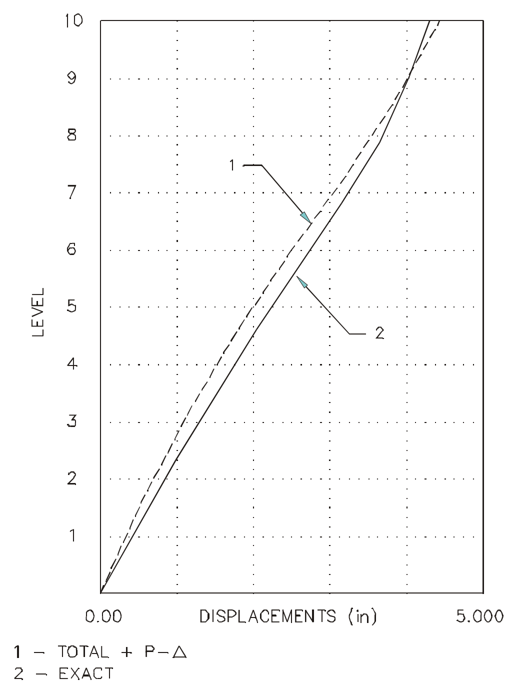

Figure 7-34. “Exact” versus approximate displacements for the 10 story frame after drift design.

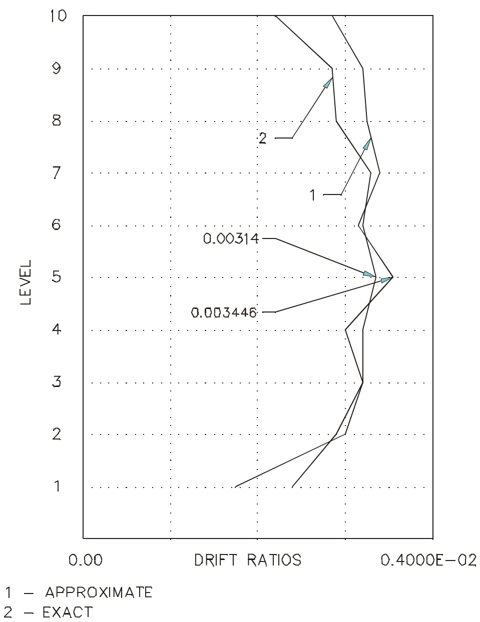

Figure 7-35. "Exact" versus approximate interstory drift ratios for the 10 story frame after drift design.

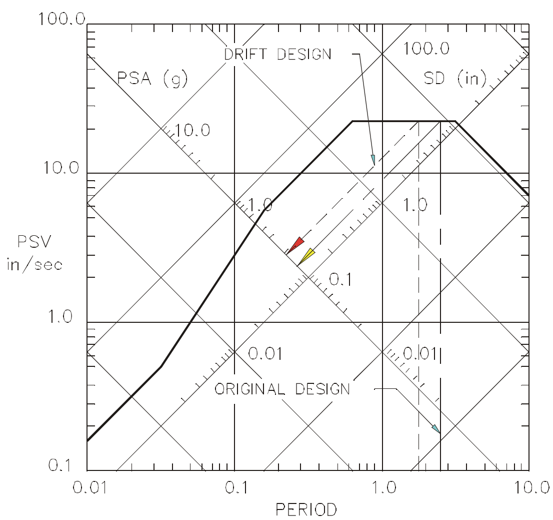

Figure 7-36. Influence of drift design on imposed inertial forces.

In reality, however, increasing member sizes for drift control, increases the stiffness of the structure and reduces its natural periods. In multistory buildings, reduction of natural periods usually implies an increase in the inertial forces exerted on the structure. Therefore, the adequacy of the modified design to withstand increased inertial forces should be examined.

Let us assume that the design ground motion for this example is represented by the design spectrum shown in Figure 7-37. Application of the Rayleigh method, or a simple dynamic analysis, reveals that the fundamental period of the original design (Figure 7-14) is about 2.7 seconds. The fundamental period of vibration of the structure after drift design (Figure 7-32) is about 1.9 seconds. Given the design spectrum of Figure 7-37, the spectral acceleration corresponding to the first mode of vibration of the structure, is about 0.15g for the original design and 0.20g for the modified design. Hence, the modified design will be expected to withstand about 33% more inertial forces than the original one.

7.5.2 Drift Design of Braced Frames

Lateral displacements of braced frames are primarily caused by two actions: deformation of the braces, and axial deformation of the columns (chord action). Several methods are available for estimation of braced frame displacements [7-44, 7-49, 7-50]. The contribution of brace deformations to story drift may be estimated by[7-44]:

$$S_{br} = \sum \frac{A_{br} E \cos^2 \alpha}{L_{br}} \qquad (7\text{-}55)$$

$$\Delta_{br} = \frac{\Sigma V}{S_{br}} \qquad (7\text{-}56)$$

where Δ_{br} is story drift due to brace deformations, ΣV is the story shear, S_{br} is the sum of stiffnesses of the braces at the level under consideration, E is the modulus of elasticity of brace, A_{br} and L_{br} are the cross sectional area and the length of each brace, and α is the angle that a brace makes with the horizontal axis. The summation is carried out over all braces at the level under consideration. Equation 7-55 is valid as long as the braces do not yield or buckle.

For ordinary braced frames, the bent story stiffness is negligible in comparison with the brace stiffness. However, in cases where rigid beam-column connections are utilized (such as eccentrically braced frames) the bent stiffness can be significant. In these situations, the bent story stiffness (see Sec. 7.5.1, "Bent Displacements") should be added to the brace stiffness.

The cantilever drifts may be computed via the Moment Area Method as explained in Sec. 7.5.1, "Cantilever Displacements". Note that in ordinary braced frames, where beams and columns are not joined by moment connections, only some of the columns (those in the vicinity of braces) provide significant resistance to cantilever deflections.

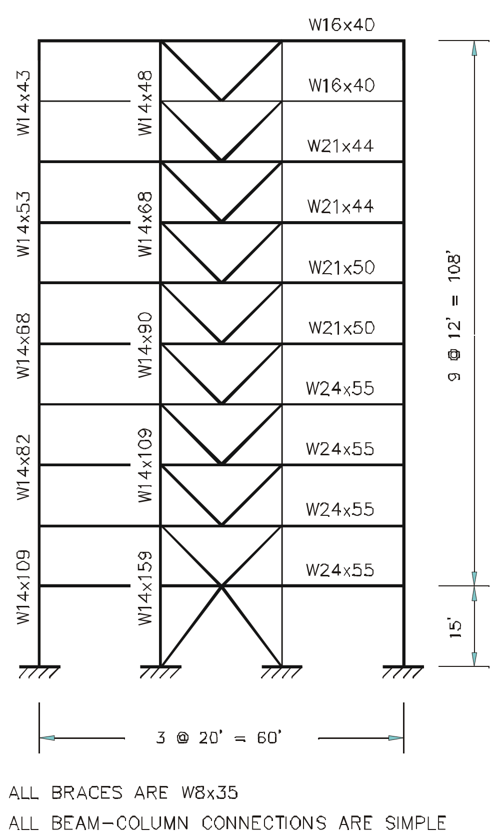

Figure 7-37. Braced frame elevation (Example 7-9).

EXAMPLE 7-9

Estimate the first and second-order lateral displacements and story drifts for the 10-story braced steel frame shown in Figure 7-38. All beam to column connections are simple. The tributary width of the frame is 30 ft. The gravity load is 100 psf on the roof level and 120 psf on typical floors. Assume that the braces are so proportioned that none of them either yield or buckle under the given loads.

We have

W8×35 $\qquad A = 10.3 \text{ in}^2$

For braces at typical floors,

$$L_{br} = \sqrt{(10)^2 + (12)^2} = 15.62 \text{ ft.} = 187.44 \text{ in.}$$

$$\cos\alpha = 10/15.62 = 0.6402$$

$$S_{br} = \sum E \frac{A_{br}}{L_{br}} \cos^2\alpha$$

$$= 2(29000)(10.3)(0.6402)^2/187.44$$

$$= 1306.27 \text{ kips/in.}$$

For braces at the first floor,

$$L_{br} = \sqrt{(10)^2 + (15)^2} = 18.03 \text{ ft.} = 216.33 \text{in.}$$

$$\cos\alpha = 10/18.03 = 0.5547$$

$$S_{br} = \frac{2(29000)(10.3)(0.5547)^2}{216.33} = 849.67 \text{ kips/in.}$$

The brace action story drifts and lateral displacements are calculated in Table 7-10. To show the accuracy of the above simple procedure, an exact first-order elastic analysis was also performed, in which large column areas were used to eliminate axial deformation of the columns. Results of the exact and approximate analyses are compared in Figure 7-39, where good agreement can be observed.

The chord action story drifts and lateral displacements are calculated in Table 7-11. The total drifts are magnified using the direct P-delta method in Table 7-12. The extent of contribution of each action to the lateral response of the frame is shown in Figure 7-40, where the dominance of chord action is evident. The results obtained by the above simple procedure are compared with those obtained by an exact second-order analysis in Figures 7-41 and 7-42.

Table 7-10. Calculation of brace-action story drifts and lateral displacements for the 10-story braced frame of example *7*-9.

Level	h, in.	ΣV, kips	S_{br} kips/in.	Δ_{br}, in.	Lat. disp. in.
10	144	30.22	1306	0.0231	0.8279
9	144	52.17	1306	0.0399	0.8048
8	144	71.74	1306	0.0549	0.7649
7	144	88.93	1306	0.0681	0.7100
6	144	103.76	1306	0.0794	0.6419
5	144	116.21	1306	0.0890	0.5625
4	144	126.30	1306	0.0967	0.4735
3	144	134.01	1306	0.1026	0.3768
2	144	139.34	1306	0.1067	0.2742
1	180	142.31	850	0.1675	0.1675

Table 7-11. Calculation of chord-action story drifts and lateral displacements for the braced frame of Example *7*-9.

Level	h, in.	ΣV, kips	M_{ov}, in.-kips	I_{oi}, in.^{4}	A, in.^{2}	$\bar{x}$, in.	Chord disp., in.	Chord drift, in.
10	144	30.22	4,352	406,080	2.66×10^5	48.00	2.958	0.452
9	144	52.17	11,864	406,080	9.92×10^5	60.88	2.506	0.443
8	144	71.74	22,194	576,000	14.7×10^5	64.72	2.063	0.426
7	144	88.93	35,001	576,000	24.6×10^5	66.63	1.637	0.397
6	144	103.76	49,942	763,200	27.6×10^5	67.78	1.240	0.360
5	144	116.21	66,677	763,200	37.9×10^5	68.56	0.880	0.312
4	144	126.30	84,864	921,600	40.8×10^5	69.12	0.568	0.256
3	144	134.01	104,161	921,600	50.9×10^5	69.55	0.312	0.190
2	144	139.34	124,226	1,344,960	42.2×10^5	69.89	0.122	0.122
1	180	142.31	149,841	1,344,960	63.2×10^5	87.20	0.000	0.000

Table 7-12 Calculation of total first-order and second-order story drifts and lateral displacements for the braced frame of example 7-9.

Level	h, in.	ΣV, kips	ΣP, kips	Δ_1 in.	μ	$\Delta_2 = \mu\, \Delta_1$, in.	2nd-Order Disp.,in.
10	144	30.22	180	0.475	1.020	0.485	3.897
9	144	52.17	396	0.483	1.026	0.496	3.412
8	144	71.74	612	0.481	1.029	0.495	2.916
7	144	88.93	828	0.465	1.031	0.479	2.421
6	144	103.76	1044	0.439	1.032	0.453	1.942
5	144	116.21	1260	0.401	1.031	0.413	1.489
4	144	126.30	1476	0.353	1.029	0.363	1.076
3	144	134.01	1692	0.301	1.027	0.309	0.713
2	144	139.34	1908	0.229	1.022	0.234	0.404
1	180	142.31	2124	0.168	1.014	0.170	0.170

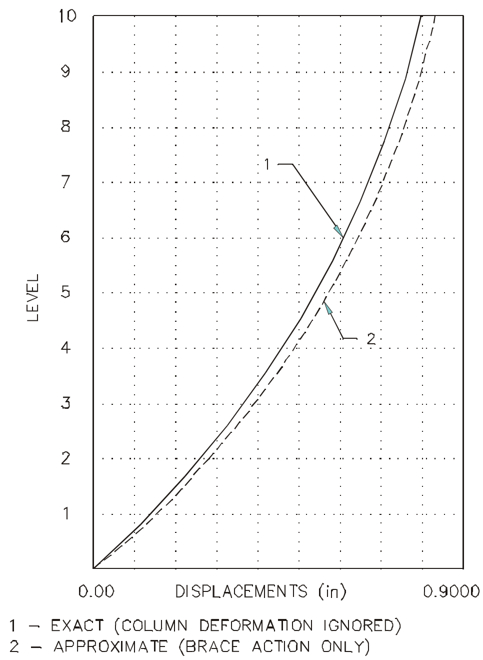

Figure 7-38. Lateral displacements caused by brace deformations.

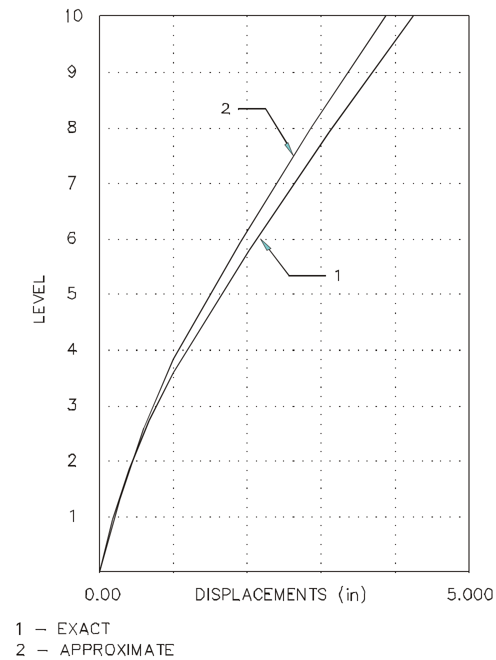

Figure 7-40. “Exact” versus approximate lateral displacements for the braced frame of example 7-9.

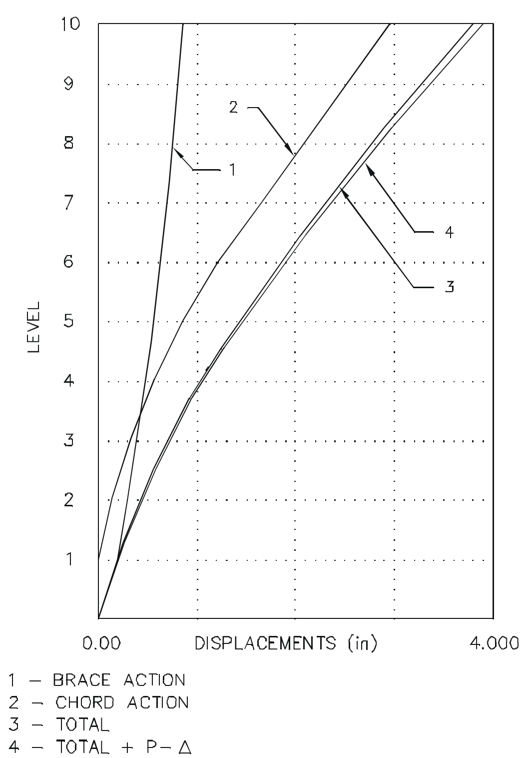

Figure 7-39. Contribution of various actions to the total lateral displacement of the braced frame of Example 7-9.

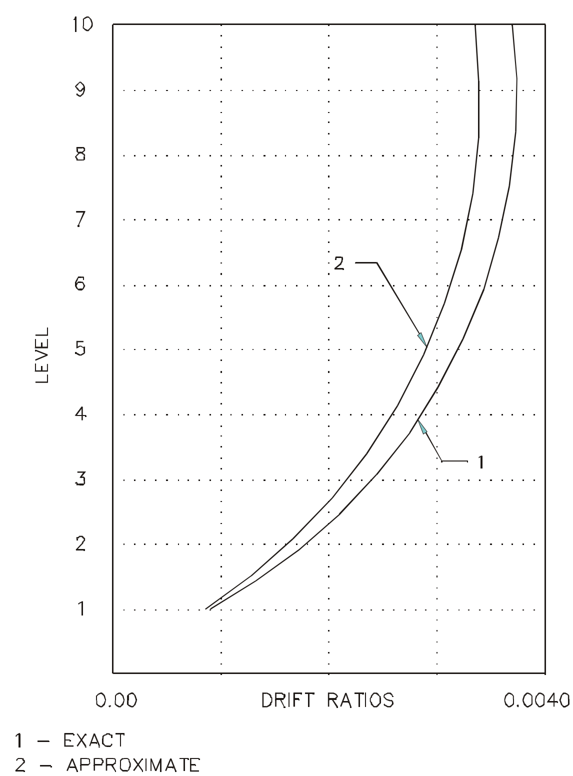

Figure 7-41. “Exact” versus approximate interstory drift ratios for the braced frame of Example 7-9.

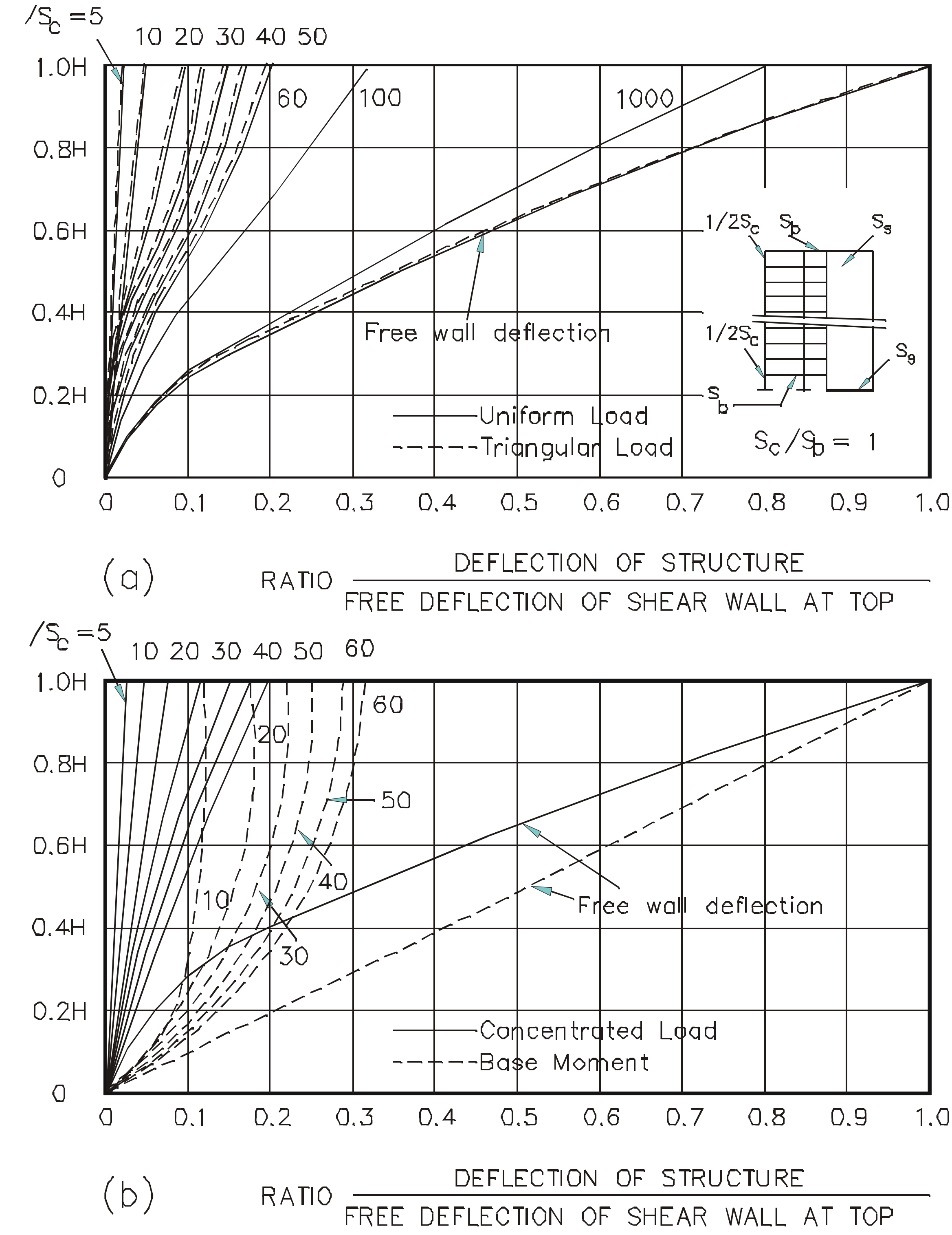

Figure 7-42. Design aid for drift design of frame-shear wall systems(7-51) (S_c/S_b=1).

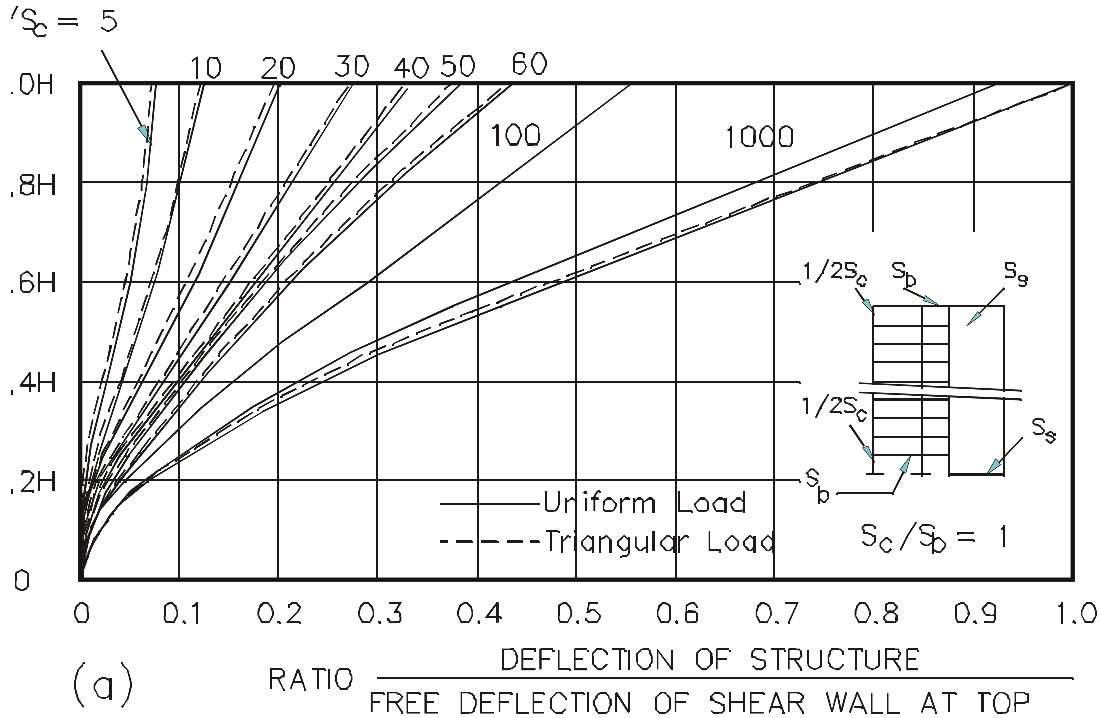

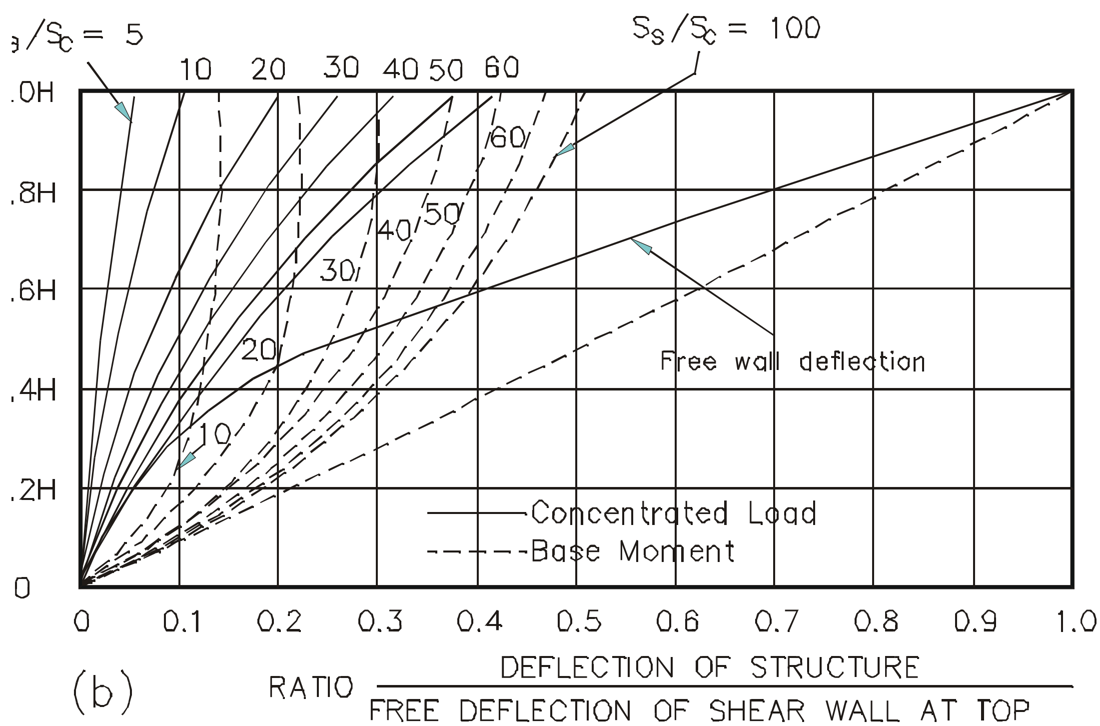

Figure 7-43. Design aid for drift design of frame-shear wall systems [7-51] (S_c/S_b=5).

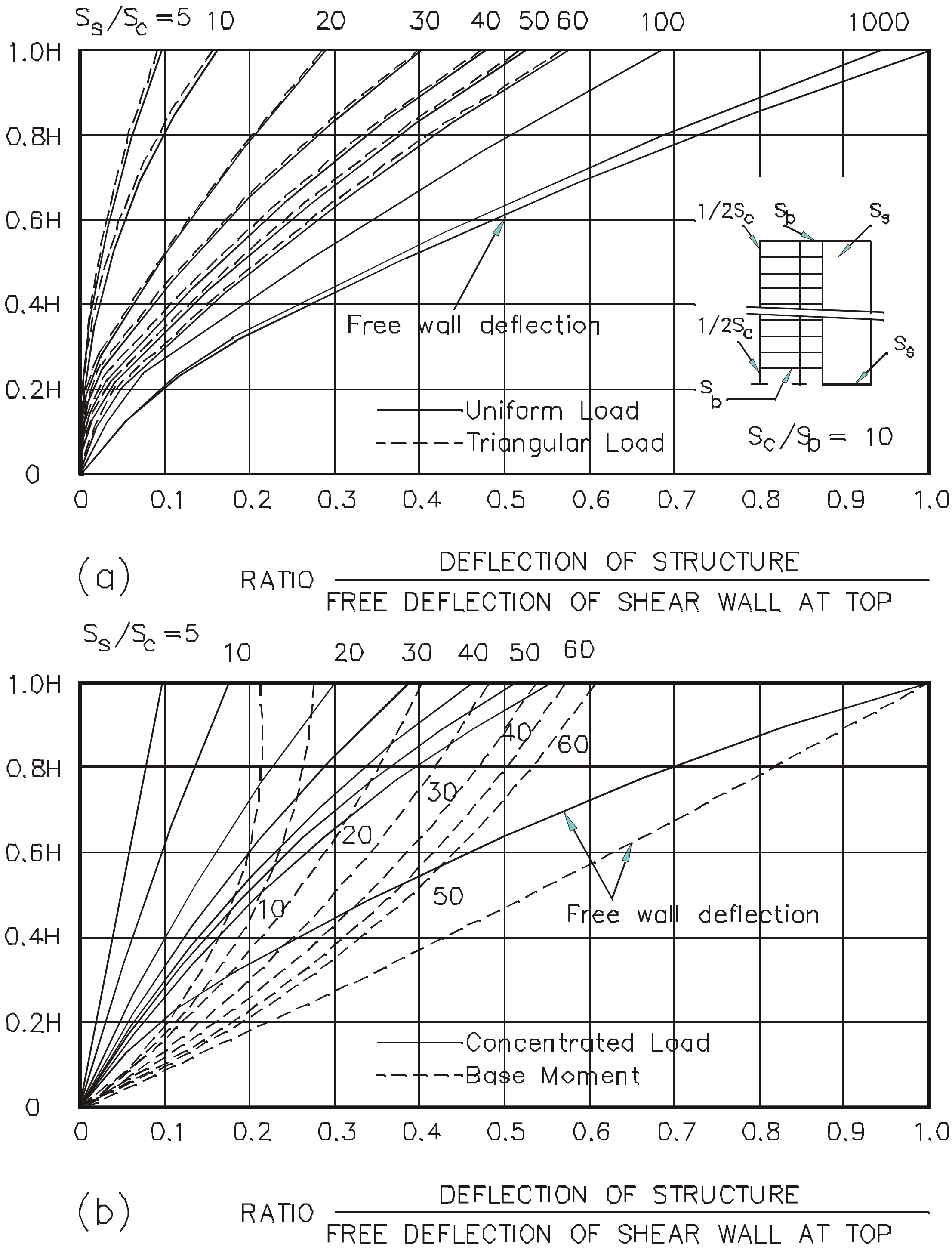

Figure 7-44. Design aid for drift design of frame-shear wall systems[7-51] (S_c/S_b=10)

7.5.3 Drift Design of Frame - Shear Wall Systems

Estimates of the lateral displacements of Frame-Shear wall systems may be obtained using the charts developed by Khan and Sbarounis[7-51]. Some of these charts, for the case of constant stiffness over the height, are reproduced in Figures 7-43 to 7-45. A sample application of the charts is presented in Example 7-10. In order to utilize the charts, the sum of stiffnesses of beams (S_b), columns (S_c) and shear walls (S_s) should be computed by adding the corresponding *EI/L* terms.

The charts provide the ratio of the lateral deflection of the frame-shear wall system to the free deflection (at the top) of the shear wall alone. Note that the ratio of S_s/S_c should be normalized by multiplying it by $(10/N)^2$, where *N* is the number of stories in the structure.

Another method for estimating drift and natural periods of frame-shear wall systems, has been developed by Stafford Smith et al.[7-52, 7-53] The method has been shown to provide accurate estimates of lateral displacements for a variety of structural systems. It can be easily adapted to programmable calculators. It is rather tedious, however, for hand calculations.

EXAMPLE 7-10

Use the Khan and Sbarounis charts to estimate the lateral displacement at the top of the 30-story frame-shear wall building shown in Figure 7-46. Assume a uniform lateral pressure of 30psf. Story heights are 12.5 feet. Use gross concrete section properties and $E = 4000$ ksi.

Column Stiffnesses:

Col. Type	b, in.	h, in.	I, ft^4	I / L, ft^3
C1	24	24	1.333	0.1067
C2	28	28	2.470	0.1976
C3	32	32	4.214	0.3371
C4	36	36	6.750	0.5400

$$\text{Total } I/L = 4(0.1067) + 6(0.1976) + 4(0.3371) + 2(0.5400) = 4.041 \text{ ft}^3$$

Beams:

B1: $$I = \frac{(14)(36)^3}{(12)^5} = 2.625 \text{ ft}^4$$

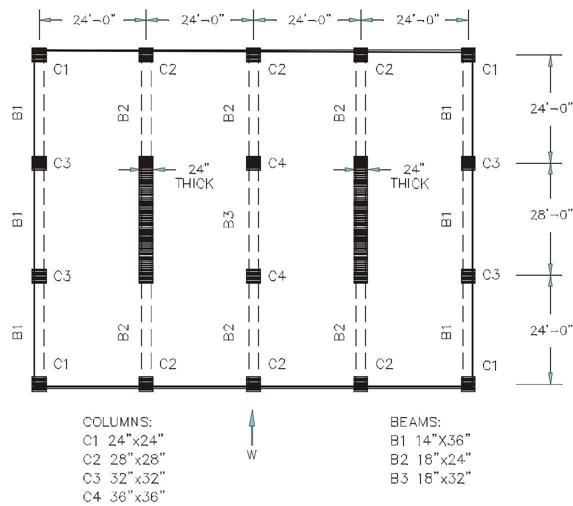

Figure 7-45. Plan of the 30 story frame-shear wall building[7-52].

B2: $$I = \frac{(18)(24)^3}{(12)^5} = 1.000 \text{ ft}^4$$

B3: $$I = \frac{(18)(32)^3}{(12)^5} = 2.370 \text{ ft}^4$$

$$\text{Total } I/L = \frac{(4)(2.625)}{24} + \frac{(2)(2.625)}{28} + \frac{(6)(1.00)}{28} + \frac{(1)(2.37)}{28} = 0.924 \text{ ft}^3$$

Walls:

$$I = \frac{(2)(28)^3}{12} = 3658.67 \text{ ft}^4$$

$$\text{Total } I/L = \frac{(2)(3658.67)}{12.5} = 585.39$$

$$\frac{S_s}{S_c} = \frac{585.39}{4.041}\left(\frac{10}{30}\right)^2 = 16.10$$

$$\frac{S_c}{S_b} = \frac{4.041}{0.924} = 4.37$$

Free deflection of the wall:

$$w = \frac{30(4)(24)}{1000} = 2.88\,\text{kips/ft}$$

$$\Delta = \frac{wl^4}{8EI} = \frac{(2.88)(375)^4}{(8)(576000)(3658.67)(2)}$$
$$= 1.69\,\text{ft.} = 20.28\,\text{in.}$$

Using the curve corresponding to $S_s/S_c = 20$ from Chart (a) of Figure 7-44, we have D_{top} = (0.22)(20.28) = 4.06 inches, which compares very well with the computed exact displacement of 4.23 inches (see Figure 7-47).

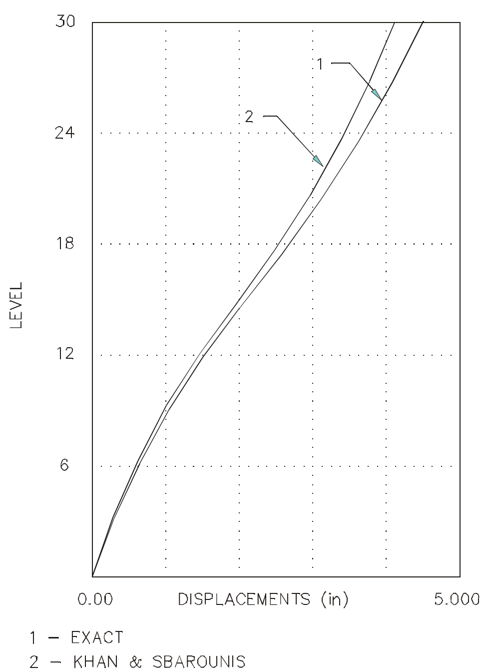

Figure 7-46. Lateral displacement of the 30 story frame-shear wall building.

7.5.4 Torsional Effects

One of the most important tasks in the process of the selection, and the subsequent proportioning, of a structural system, is the minimization of torsional response. In general, this is a rather difficult task, and its success is strongly dependent on the intuition and experience of the designer.

For buildings in which the locations and relative stiffnesses of the lateral load resisting sub-systems (e.g. frames and walls) do not vary significantly along the height, the torsional displacements may be estimated as follows:

1. For buildings which are composed of only one type of lateral load resisting system (moment frames, braced frames, or walls), the torsional rotation at the *i*th floor, θ_i, and the corresponding torsional drift of the j th frame at this floor, Δ_j, may be estimated as:

$$\theta_i = \frac{(\Sigma V_i)\, e_i^2}{J} \tag{7-57}$$

$$\Delta_j = R_j \theta_i \tag{7-58}$$

where ΣV_i is the story shear, e_i is the eccentricity of the "center of rigidity" from the center of mass, R_j is the closest distance from the *j*th frame to the center of rigidity, and J is the torsional story stiffness given by

$$J = \Sigma K_j R_j^2 \tag{7-59}$$

2. For combination systems (frame-shear wall systems, moment frame and braced frame combinations), the process is more complex:

– The direct lateral displacements and story drifts of the structure are obtained via the Khan-Sbarounis charts or any other appropriate method.
– The total direct story shear carried by the frames subjected to the above displacements, V_{fi}, are calculated (see Section 7.5.1, "Bent Displacements).
– The shear V_{fi} is distributed among the various frames according to their relative stiffness in the direction of applied load.
– The rest of the story shear (ΣV_i - V_{fi}) is distributed among the various walls (braced frames) according to their relative stiffness in the direction of applied loads.
– The shear in each frame or wall, as calculated in the two preceding steps, is used as a measure of rigidity, and the center of rigidity of the entire system is located.

– The torsional rotation and the corresponding torsional drift of individual frames and walls are calculated using Equations 7-57 and 7-58.

It may be noticed that the concept of the "center of rigidity" is of significant use in the preliminary evaluation of the torsional response. However, the physical limitations of such a concept when applied to the seismic response of general, three dimensional, multistory structures should be clearly understood. In a three dimensional, multi-story structure, if it exhibits significant plan and elevation irregularities, the lateral resistance is provided by a combination of strongly inter-dependent actions, both within a single story, and among various floors. In general, for such a complex system, centers of rigidity (points of application of forces for a torsion-free response) do not exist. Furthermore, if and when they exist, they must all lie on a single vertical line[7-54].

7.6 SEISMIC CODE REQUIREMENTS FOR DRIFT AND P-DELTA ANALYSIS

7.6.1 UBC-97 Provisions

UBC-97[7-57], addresses design for drift and lateral stiffness within the framework of strength design. The reduced lateral displacement calculated by utilizing the reduction factor, R, is called Δ_S. The maximum inelastic response displacement is called Δ_M and is calculated from

$$\Delta_M = 0.7R\Delta_S \qquad (7\text{-}60)$$

Alternatively, Δ_M may be computed by nonlinear time history analysis. The analysis to determine Δ_M must consider P-delta effects. P-delta effects, however, may be ignored when the ratio of secondary moments to first-order moments does not exceed 0.10. This ratio is calculated from

$$\theta = \frac{P_x \Delta_{Sx}}{V_x h_{sx}} \qquad (7\text{-}61)$$

where

Δ_{Sx} = story drift based on Δ_S acting between levels x and x-1

V_x = the design seismic shear force acting between levels x and x-1

h_{sx} = the story height below level x

P_x = the total unfactored vertical design load at and above level x.

In seismic zones 3 and 4, P-delta effects need not be considered when the story drift index does not exceed 0.02/R.

UBC-97 permitted drift using Δ_M is a function of the fundamental period of the structure

$$\begin{cases} \Delta_{Mx} \le 0.025 h_{sx} & \text{for } T < 0.7\,\text{sec}. \\ \Delta_{Mx} \le 0.020 h_{sx} & \text{for } T \ge 0.7\,\text{sec}. \end{cases} \qquad (7\text{-}61)$$

where

Δ_{Sx} = story drift based on Δ_M acting between levels x and x-1

The fundamental period used in drift calculations is not subject to lower-bound period formulas of the code (see Chapter 4) and may be based on the Rayleigh formula or other rational calculations such as a detailed computer model of the structure. Furthermore, UBC-97 permits these drift limits to be exceeded when the engineer can demonstrate that greater drift can be tolerated by both structural and nonstructural elements whose performance can affect the seismic safety of the structure. Therefore, if local drift is exceeded locally in an area without a serious seismic ramification, it can be tolerated and there is no need for a redesign.

7.6.2 IBC-2000 Provisions

The provisions of IBC-2000[7-58] embody a convergence of the efforts initiated by the Applied Technology Council's ATC 3-06[7-59] document published in 1978 and its successive modifications by the Federal Emergency Management Agency[7-60] and that of the UBC provisions. Therefore, setting aside the difference in the language and vocabulary, IBC-2000 and UBC-97 drift and P-delta provisions are very similar [7-60]. Quite rationally, IBC-2000 addresses seismic design for drift and lateral stiffness exclusively at the ultimate limit state of building behavior.

According to IBC-2000 provisions, the design story drift, Δ, is computed as the difference of the deflections, δ_x, at the top and bottom of the story under consideration in accordance with the following formula

$$\delta_x = \frac{C_d \delta_{xe}}{I_E} \tag{7-62}$$

where:

C_d = the deflection amplification factor as given in Table 5-17,

δ_{xe}.= the deflection determined by an elastic analysis of the force-resisting system, and

I_E = the occupancy importance factor as given in Section 5.4.2.

The maximum inter-story drift index calculated using Equation 7-62 should not exceed the corresponding limits described in Section 5.4.15. Furthermore, for structures assigned to seismic design categories *C*, *D*, *E*, or *F* having plan irregularity types 1a or 1b (see Chapter 5) the design story drift is to be computed as the largest difference of the deflections along any of the edges of the structure at the top and bottom of the story under consideration.

To determine whether a P-delta analysis is required, a stability coefficient is used. This is in fact, the same as the stability index introduced previously in this Chapter. P-delta effects need not be considered when the stability coefficient, θ as determined from Equation 7-63 is less than 0.10:

$$\theta = \frac{P_x \Delta}{V_x h_{sx} C_d} \tag{7-63}$$

where

Δ = the design story drift

V_x = the seismic shear force acting between level x and x-1

h_{sx} = the story height below level x, and

P_x = the total unfactored vertical design load at and above level x.

The stability coefficient, θ, should not exceed an upper limit of θ_{max} given as

$$\theta_{\max} = \frac{0.5}{\beta C_d} \le 0.25 \tag{7-63}$$

where:

β = the ratio of shear demand to shear capacity for the story between level x and x-1. If this ratio is not calculated, a value of $\beta = 1$ should be used.

When θ is greater than 0.10 but less than θ_{max}, IBC-2000 permits direct calculation of P-delta effects in a manner very similar to the direct P-delta method discussed earlier in this Chapter. That is, the calculated first-order interstory drifts are to be multiplied by a factor of $1/(1-\theta)>1$. If, however, θ is larger than θ_{max} the structure is potentially unstable and should be redesigned.

REFERENCES

7-1 Council on Tall Buildings, Committee 16, "Stability," Chapter SB-4, Vol. SB of *Monograph on Planning and Design of Tall Buildings*, ASCE, New York, 1979.

7-2 Scholl, R.E. (ed), "Effects Prediction Guidelines for Structures Subjected to Ground Motion," Report No. JAB-99-115, URS/Blume Engineers, San Francisco, 1975.

7-3 Scholl, R.E., "Brace Dampers: An Alternative Structural System for Improving the Earthquake Performance of Buildings," *Proceedings of the 8th World Conference on Earthquake Engineering*, San Francisco, Vol 5., Prentice Hall, 1984.

7-4 Ohta, Y., and Omote, S., "An Investigation into Human Psychology and Behavior During an Earthquake," *Proceedings of the 6th World Conference on Earthquake Engineering*, India, 1977.

7-5 Mileti, D.S., and Nigg, J.M., "Earthquakes and Human Behavior," *Earthquake Spectra*, EERI, Vol. 1, No. 1, Feb., 1984.

7-6 Durkin, M.E., "Behavior of Building Occupants in Earthquakes," *Earthquake Spectra*, EERI, Vol. 1, No. 2, Feb., 1985.

7-7 Chen, W.F., and Lui, E.M., *Structural Stability*, Elsevier Science Publishing Company, New York, 1987.

7-8 Wakabayashi, M., *Design of Earthquake Resistant Buildings*, MacGraw Hill, New York, 1986.

7-9 Rosenblueth, E., "Slenderness Effects in Buildings," *Journal of the Structural Division*, ASCE, Vol. 91, No. ST1, Proc. Paper 4235, January, 1967, pp. 229-252.

7-10 Stevens, L. K., "Elastic Stability of Practical Multi-Story Frames*," Proceedings, Institution of Civil Engineers*, Vol. 36, 1967, pp. 99-117.

7-11 Goldberg, J. E., "Approximate Methods for Stability and Frequency Analysis of Tall Buildings," *Proceedings, Regional Conference on Tall Buildings*, Madrid, Spain, September, 1973, pp. 123-146.

7-12 Council on Tall Buildings, Committee 23, "Stability," Chapter CB-8, Vol. CB of *Monograph on Planning and Design of Tall Buildings*, ASCE, New York, 1978.

7-13 Singh, J.P., "Earthquake Ground Motions: Implications for Designing Structures and Reconciling Structural Damage," *Earthquake Spectra*, EERI, Vol. 1, No. 2, Feb., 1985.

7-14 Naeim, F., "On Seismic Design Implications of the 1994 Northridge Earthquake Records*," Earthquake Spectra*, EERI, Vol. 11, No. 1, Feb. 1995.

7-15 Anderson, J.C., and Bertero, V.V., "Uncertainties in Establishing Design Earthquakes," *Proceedings of a two-day Course from EERI on Strong Ground Motion*, San Francisco and Los Angeles, Apr., 1987.

7-16 MacGregor, J.G, and Hage, S.E., "Stability Analysis and Design of Concrete Frames," *Journal of the Structural Division*, ASCE, Vol. 103, No. ST10, October, 1977, pp. 1953-1970.

7-17 Wynhoven, J.H., and Adams, P.F., "Behavior of Structures Under Loads Causing Torsion," *Journal of the Structural Division*, ASCE, Vol. 98, No. ST7, July, 1972, pp. 1361-1376.

7-18 Salmon, C.G., and Johnson, J.E., *Steel Structures, Design and Behavior*, 2nd Edition, Harper and Row, 1980, pp. 843-851.

7-19 Johnston, B.G. (ed.), *Structural Stability Research Council, Guide to Stability Design Criteria for Metal Structures*, 3rd Edition, John Wiley and Sons, New York, 1976.

7-20 Cheong-Siat-Moy, F., "Frame Design Without Using Effective Column Length," *Journal of the Structural Division*, ASCE, Vol. 104, No. ST1, Jan., 1978, pp. 23-33.

7-21 Cheong-Siat-Moy, F., "K-Factor Paradox," *Journal of Structural Engineering*, ASCE, Vol. 112, No. 8, Aug., 1986, pp. 1747-1760.

7-22 Nair, R. S., "A Simple Method of Overall Stability Analysis for Multistory Buildings," *Developments in Tall Buildings* - 1983, Council on Tall Buildings and Urban Habitat, Lynn S. Beedle (Editor-in-Chief), Van Nostrand Reinhold, New York, 1983.

7-23 Nair, R.S., "Overall Elastic Stability of Multistory Buildings," *Journal of the Structural Division*, ASCE, Vol. 101, No. ST12, Dec., 1975, pp. 2487-2503.

7-24 Springfield, J., and Adams, P.F., "Aspects of Column Design in Tall Steel Buildings," *Journal of the Structural Division*, ASCE, Vol. 98, No. ST5, May, 1972, pp. 1069-1083.

7-25 Wood, B.R., Beaulieu, D., and Adams, P.F., "Column Design by P-Delta Method," *Journal of the Structural Division,* ASCE, Vol. 102, No. ST2, Feb., 1976, pp. 411-427.

7-26 Lai, S.A., and MacGregor, J.G., "Geometric Nonlinearities in Unbraced Multistory Frames," *Journal of Structural Engineering*, ASCE, Vol. 109, No. 11, Nov., 1983, pp. 2528-2545.

7-27 Nixon, D., Beaulieu, D., and Adams, P.F., "Simplified Second-Order Frame Analysis," *Canadian Journal of Civil Engineering*, Vol. 2, No. 4, Dec., 1975, pp. 602-605.

7-28 Renton, J.D., "Stability of Space Frames by Computer Analysis," *Journal of the Structural Division*, ASCE, Vol. 88, No. ST4, Aug., 1962, pp. 81-103.

7-29 Chu, K.H., and Rampetsreiter, R.H., " Large Deflection Buckling of Space Frames," *Journal of the Structural Division,* ASCE, Vol. 98, No. ST12, Dec., 1972, pp. 2701-2722.

7-30 Connor, J.J., Jr., Logcher, R.D., and Chen, S.C., "Nonlinear Analysis of Elastic Frame Structures," *Journal of the Structural Division*, ASCE, Vol. 94, No. ST6, Jun., 1968, pp. 1525-1547.

7-31 Zarghammee, M.S., and Shah, J.M., "Stability of Space Frames," *Journal of the Engineering Mechanics Division*, ASCE, Vol. 94, No. EM2, Apr., 1968, pp. 371-384.

7-32 Krajcinovic, D., "A Consistent Discrete Elements Technique for Thin-Walled Assemblages," *International Journal of Solids and Structures*, Vol. 5, 1969, pp. 639-662.

7-33 Barsoum, R.S., and Gallagher, R.H., "Finite Element Analysis of Torsional Flexural Stability Problems," *International Journal for Numerical Methods in Engineering*, Vol. 2, 1970, pp. 335-352.

7-34 Bazant, Z.P., and El Nimeiri, M., "Large-Deflection Buckling of Thin Walled Beams and Frames," *Journal of the Engineering Mechanics Division*, ASCE, Vol. 79, No. EM6, Dec., 1973, pp. 1259-1281.

7-35 Yoo, C.H., "Bimoment Contribution to Stability of Thin-Walled Assemblages," *Computers and Structures*, Vol. 11, 1980, pp. 465-471.

7-36 Yang, Y., and McGuire, W., "Stiffness Matrix for Geometric Nonlinear Analysis," *Journal of Structural Engineering*, ASCE, Vol. 112, No. 4, Apr., 1986, pp. 853-877.

7-37 Naeim, F., *An Automated Design Study of the Economics of Earthquake Resistant Structures*, Ph.D. Dissertation, Department of Civil Engineering, University of Southern California, Aug., 1982.

7-38 Neuss, C.F., Maison, B.F., and Bouwkamp, J.G., *A Study of Computer Modeling Formulation and Special Analytical Procedures for Earthquake Response of Multistory Buildings*, A Report to National Science Foundation," J.G. Bouwkamp, Inc., Berkeley, California, Jan., 1983, pp. 335-362.

7-39 Wilson, E.L., and Habibullah, A., "Static and Dynamic Analysis of Multi-Story Buildings Including the P-Delta Effects," *Earthquake Spectra*, EERI, Vol.3, No.2, May, 1987.

7-40 Freeman, S.A., Czarncki, R.M., and Honda, K.K., "Significance of Stiffness Assumptions on Lateral Force Criteria," in *Reinforced Concrete Structures Subjected to Wind and Earthquake Forces*, Publication SP-63, American Concrete Institute, Detroit, Michigan, 1980.

7-41 Wong, C.H., El Nimeiri, M.M., and Tang, J.W., "Preliminary Analysis and Member Sizing of Tall Tubular Steel Buildings," *AISC Engineering Journal*, American Institute of Steel Construction, Second Quarter, 1981, pp. 33-47.

7-42 Council on Tall Buildings, Committee 14, "Elastic Analysis and Design," Chapter SB-2, Vol. SB of *Monograph on Planning and Design of Tall Buildings*, ASCE, New York, 1979.

7-43 Cheong-Siat-Moy, F., "Multistory Frame Design Using Story Stiffness Concept*," Journal of the Structural Division*, ASCE, Vol. 102, No. ST6, Jun., 1976, pp. 1197-1212.

7-44 Cheong-Siat-Moy, F., "Consideration of Secondary Effects in Frame Design," *Journal of the Structural Division*, ASCE, Vol. 103, No. ST10, Oct., 1977, pp. 2005-2019.

7-45 Krawinkler, H., Bertero, V.V., and Popov, E.P., *Inelastic Behavior of Steel Beam-to-Column Subassemblages*, Earthquake Engineering Research Center, University of California, Berkeley, Report No. EERC 71-7, Oct., 1971.

7-46 Becker, E.R., *Panel Zone Effect on the Strength and Stiffness of Rigid Steel Frames*, Structural Mechanics Laboratory Report, University of Southern California, Jun., 1971.

7-47 Richards, R.M., and Pettijohn, D.R., *Analytical Study of Panel Zone Behavior in Beam-Column Connections*, University of Arizona, Nov., 1981.

7-48 Slutter, R.G., *Tests of Panel Zone Behavior in Beam-Column Connections*, Fritz Engineering Laboratory, Lehigh University, Report No. 200-81-403-1, 1981.

7-49 Teal, E.J., *Practical Design of Eccentric Braced Frames to Resist Seismic Forces*, Structural Steel Educational Council.

7-50 White, R.N., and Salmon, C.G., (eds), *Building Structural Design Handbook*, John Wiley and Sons, New York, 1987.

7-51 Khan, F.R., and Sbarounis, J.A., " Interaction of Shear Walls and Frames," *Journal of the Structural Division*, ASCE, Vol. 90, No. ST3, Jun., 1964, pp. 285-335.

7-52 Stafford Smith, B., Kuster, M., and HoenderKamp, J.C.D., "Generalized Method for Estimating Drift in High-Rise Structures," *Journal of Structural Engineering*, ASCE, Vol. 110, No. 7, Jul., 1984, pp. 1549-1562.

7-53 Stafford Smith, B., and Crowe, E.,"Estimating Periods of Vibration of Tall Buildings," *Journal of Structural Engineering*, ASCE, Vol. 112, No. 5, May, 1986, pp. 1005-1018.

7-54 Riddell, R., and Vasques, J.,"Existence of Centers of Resistance and Torsional Uncoupling of Earthquake Response of Buildings," *Proceedings of the 8th World Conference on Earthquake Engineering*, San Francisco, Vol 5., Prentice Hall, 1984.

7-55 International Conference of Building Officials, *Uniform Building Code -1997*, Whittier, California, 1997.

7-56 International Code Council*, International Building Code 2000*, Falls Church, Virginia, 2000.

7-57 Applied Technology Council, *Tentative Provisions for the Development of Seismic Regulations for Buildings*, Publication ATC-3-06, 1978.

7-58 Federal Emergency Management Agency, *1997 Edition of NEHRP Recommended Provisions for the Development of Seismic Regulations for New Buildings*, 1997.